Two Dimensional topological states in Zinc Blende heterostructures.

Gorm Ole Steffensen
Qbv806@alumni.ku.dk
Bachelor project in physics
Niels Bohr Institutet University of Copenhagen
Supervisor: Karsten Flensberg

10/06/2015

1 Abstract

In this thesis we have investigated the topological insulating state in zinc blende heterostructures. We find that by varying thickness one can tune a normal band structure into an inverted band structure. By use of $k \cdot p$ and envelope function theory we obtain the band structure of two quantum wells. The HgTe well is solved by neglecting spurious solutions and we obtain an inverted band structure in the regime 6.7nm$< L <$ 8.66nm. By use of Foreman's ordering and scattering matrices we derive the band structure of the InAsGaSb quantum well and obtain an inverted band structure in the regime 8.7nm$< d <$ 14.5nm. We then develop the BHZ Hamiltonian for HgTe in the inverted regime to obtain time reversal protected helical edge states. Finally we discuss transport measurements which can verify the existence of helical edge states and we conclude that we can achieve the quantum spin hall effect in the HgTe quantum wells.

Contents

2 Introduction

Within that last couple of years the topological insulating state has been proposed and realized [2][1]. This new state of matter supports the existence of edge states without breaking time reversal symmetry. In the topological insulating state one finds an odd number of Kramer's pairs at open interfaces. These helical edge states leads to novel transport effects such as the quantum spin hall phase [7].

The first verified topological insulator was the inverted HgTe quantum well [1]. Recently the InAsGaSb broken gap quantum well have also been proposed as a topological insulator [5] and verified experimentally [22]. New transport measurements of weird magneto-resistance makes development of effective models a essential part of understanding this new phase [19].

In this thesis we will investigate the topological state in zinc blende heterostrucutres. The purpose of this work is to find inverted regimes in different quantum wells in order to achieve the topological insulating state. In this regime we wish to obtain effective Hamiltonians describing the bands interactions. We will then develop and investigate the helical edge states located at open interfaces. In order to achieve this we need to derive an effective Hamiltonian for zinc blende crystals and find proper boundary conditions for heterostructurs.

3 $k \cdot p$ approximation

Using symmetry arguments and $k \cdot p$ theory we will here develop a second order Hamiltonian describing the interactions between the conduction band and the valence band. These deviations are based on the work of [11] and [9]. First we define the principal elements of this theory.

Since the crystal is invariant to any discrete translations composed of lattice vectors we express our wavefunction in terms of Bloch waves

$$\psi(r) = e^{ik\cdot r}u(k,r) \Rightarrow \psi(r+G) = e^{ik\cdot(r+G)}u(k,r). \tag{3.1}$$

Here $u(k,r)$ is a function periodic with G and G is composed of linear combinations of lattice vectors. We insert this into the Schrödinger equation and obtain

$$H\psi = \left[\frac{p^2}{2m_0} + V(k,r)\right]\psi \Rightarrow Hu(k,r) = \left[\frac{p^2}{2m_0} + \frac{\hbar^2k^2}{2m_0} + \frac{\hbar k\cdot p}{m_0} + V(k,r)\right]u(k.r). \tag{3.2}$$

which we separate into k dependent terms and k independent terms. The k independent terms describe the electrons energy due to motion around the atoms while the k dependent terms describe the wave packet moving as a whole. The k independent terms determines the energy of the band at the $k = 0$ point:

$$\left[\frac{p^2}{2m_0} + V(k,r)\right]u(k,r) = E_0u(k,r). \tag{3.3}$$

In order to develop an effective theory we need to do perturbations around the $k \cdot p$ term from Eq.3.2. We will use group theory to identify which terms that are non zero. A quick review and explanation of group theory for the zinc blend crystal is provided in appendix A. Here we will just present the character table for the point group T_d to which the zinc blende crystal belongs:

In the type of semiconductors we are interested in the valence band is composed of atomic p orbitals, while the conduction band is made of s orbitals and the Fermi energy is centered between these orbitals. The s orbitals are fully symmetric and therefore invariant under all transformations, since transformations consist of rotations or reflections. Therefore they belong to the Irreducible Representation (IRR) $\Gamma 1$. p orbitals are atomic orbitals that are anti-symmetric in one direction. They are triply degenerate and must be described by a 3 dimensional IRR. Using a antisymmetric basis x, y and z we have already constructed a matrix for S_4 with trace -1 (Eq.A.1). So since the p states are triply degenerate and must have the character -1 for S_4 we see from table.1 that they belong to the IRR $\Gamma 4$. Since they transform as the basis x, y and z we label them with Cartesian coordinates.

	E	$3C_2$	$6S_4$	6σ	$8C_3$
$\Gamma 1$	1	1	1	1	1
$\Gamma 2$	1	1	-1	-1	1
$\Gamma 3$	2	2	0	0	-1
$\Gamma 4$	3	-1	-1	1	0
$\Gamma 5$	3	-1	1	-1	0

Table 1: Character table for point group T_d

Other states belonging to the rest of the IRR and more distant p and s bands will only be treated as perturbations to the p and s states near the Fermi surface.

We derive Lowdin's perturbation theory which allows us to treat distant bands as perturbations. First we split the states into two groups: A and B. Where A are the bands close to the Fermi surface and B are the distant bands treated only as perturbations [11]. We define a Hamiltonian with a approximate set of orthogonal eigenstates:

$$H\psi = E\psi \quad \text{and} \quad \psi = \sum_n c_n \psi_n^0. \tag{3.4}$$

In our work, these eigenstates would correspond to zone-center wavefunctions for different bands. We insert the approximate set and multiply the left side with ψ_m^0 to obtain

$$\sum_n c_n \left\langle \psi_m^0 \right| H \left| \psi_n^0 \right\rangle = c_m E. \tag{3.5}$$

Defining $\left\langle \psi_m^0 \right| H \left| \psi_n^0 \right\rangle = H_{mn}$ and removing state m from the summation leaves us with

$$\sum_{n \neq m} c_n H_{mn} = c_m(E - H_{mm}) \Rightarrow c_m = \sum_{n \neq m} \frac{c_n H_{mn}}{E - H_{mm}}, \tag{3.6}$$

which we separate into sums for states A and B. Latin indices span the subset A and greek the subset B. Considering the case of m belonging to A and m belonging to B independently yields

$$c_m = \sum_{n \neq m} \frac{c_n H_{mn}}{E - H_{mm}} + \sum_{\alpha} \frac{c_\alpha H_{m\alpha}}{E - H_{\alpha\alpha}} \quad \text{and} \quad c_\alpha = \sum_{\alpha} \frac{c_n H_{\alpha n}}{E - H_{\alpha\alpha}} + \sum_{\beta \neq \alpha} \frac{c_\beta H_{\alpha\beta}}{E - H_{\beta\beta}}. \tag{3.7}$$

We then use an iterative procedure where we insert c_α into the equation for c_m to obtain a perturbative approximation. We multiply by $E - H_{mm}$ and insert H_{mm} back into summation we get

$$Ec_m = \sum_n H_{mn} c_n + \sum_{\alpha n} \frac{H_{m\alpha} H_{\alpha n}}{E - H_{\alpha\alpha}} c_n + \sum_{\alpha\beta, \beta \neq \alpha} \frac{H_{m\alpha} H_{\alpha\beta}}{E - H_{\alpha\alpha}} c_\beta \tag{3.8}$$

By pulling out c_n and ignoring the rest we would have up to second order perturbation. By continuing insertion of Eq.3.7 into the third term we would obtain higher order perturbations. So up to second order

$$H_{mn}^{(2)} = H_{mn} + \sum_{\alpha} \frac{H_{m\alpha} H_{\alpha n}}{E - H_{\alpha\alpha}}. \tag{3.9}$$

The next challenge is then to identify which terms that contribute to this sum. Group theory provides an easy way of finding terms of $H_{mn}^{(2)}$ that are zero. We do this by utilizing selection rules.

Treating the $k \cdot p$ term as a perturbation with k as a vector and p as a operator we want to calculate terms of the form

$$Pk = \langle \Psi_2 | \, p \, | \Psi_1 \rangle \, k. \tag{3.10}$$

with Ψ_n as a set of degenerate eigenfunctions of the Hamiltonian that transforms according to an Irreducible representation (IRR). Now lets assume that Ψ_1 belongs to the IRR $\Gamma 4$ and since the momentum operator transforms the same way as x, y and z we know that p must also transform as $\Gamma 4$. Taking the product between them would therefore result in nine new wave functions generating a new representation. This representation would then be tensor product $\Gamma 4 \otimes \Gamma 4$.

This corresponds to every matrix representations of each IRR being multiplied together. So by taking the trace we obtain:

$$\sum_{\mu\mu'} D^j_{\mu\mu}(A) D^i_{\mu'\mu'}(A) = \sum_{\mu\mu'} D^i_{\mu\mu}(A) D^i_{\mu'\mu'}(A) \Rightarrow \chi_i^1 \chi_i^2. \tag{3.11}$$

The last index on χ is just to indicate that even though the χ's belong to the same symmetry operator, they can have different characters in different IRR.

Now lets assume that this new representation is reducible. Then the characters of this representation would consist of the sum of the characters of the IRR since characters are defined as the trace.

So if we could guess the combinations of characters from IRRs that ad up to the characters of the new representation we would have reduced it to irreducible form. This method is easily applied if the group does not consist of a huge number of IRRs. In our example a look at the table.1 shows that

$$\Gamma 4 \otimes \Gamma 4 = \Gamma 1 \oplus \Gamma 3 \oplus \Gamma 4 \oplus \Gamma 5. \tag{3.12}$$

Where the direct sum is the way of combining different IRR into a single representation. Now this representation must also have a set of basis functions which we call Ψ_3. So Eq.3.10 reduces to

$$Pk = \langle \Psi_2 | \Psi_3 \rangle \, k, \tag{3.13}$$

and since basis vectors from different IRR are orthogonal to each other this equation will only have a value if the IRR corresponding to $\Gamma 2$ is one of the 4 IRRs of Eq.3.12. So for the p and s bands we have the selection rules

$$\Gamma 4 \otimes \Gamma 4 = \Gamma 1 \oplus \Gamma 3 \oplus \Gamma 4 \oplus \Gamma 5 \quad \text{and} \quad \Gamma 4 \otimes \Gamma 1 = \Gamma 4, \tag{3.14}$$

so to first order the interaction between s and p orbitals is given by

$$\frac{\hbar}{m_0} \sum_{i,j} \langle s | \, p_i \, | j \rangle \, k_i = \frac{\hbar}{m_0} \langle s | \, p_i \, | i \rangle \, k_i = Pk_i. \tag{3.15}$$

Where i and j are the coordinates x, y and z and where we used the following pairing rule: since our group contains the symmetry C_2 which changes sign of 2 axis's and leaves 1 unchanged, all terms that contains unpaired (antisymmetric) terms of x, y and z will be 0. These terms must have equal strength since they are invariant under symmetry operations. To first order we then have the following Hamiltonian:

$$H_k \, |\Psi\rangle = \begin{bmatrix} E_c + \frac{\hbar^2 k^2}{2m_0} & Pk_x & Pk_y & Pk_z \\ Pk_x & E_v + \frac{\hbar^2 k^2}{2m_0} & 0 & 0 \\ Pk_y & 0 & E_v + \frac{\hbar^2 k^2}{2m_0} & 0 \\ Pk_z & 0 & 0 & E_v + \frac{\hbar^2 k^2}{2m_0} \end{bmatrix} \begin{bmatrix} s \\ x \\ y \\ z \end{bmatrix}. \tag{3.16}$$

Where P is known as the Kane parameter and the matrix is known as the 4×4 Kane Hamilton. This Hamilton is inversion symmetric since parity changes sign of p states but leaves s states unchanged.

3.1 Second order perturbations

We will now consider second order terms from Lowdin's perturbation Eq.3.9. These terms are corrections from the distant bands B to bands A. We will encounter 4 different terms. The first contribution is,

$$\frac{\hbar^2}{m_0^2} \sum_{n,i,j} \frac{\langle s | \, p_i \, | n \rangle \langle n | \, p_j \, | s \rangle}{E_c - E_n} k_i k_j = \frac{\hbar^2}{m_0^2} \sum_{n,i} \frac{\langle s | \, p_i \, | n \rangle \langle n | \, p_i \, | s \rangle}{E_c - E_n} k_i^2 = A(k_x^2 + k_y^2 + k_z^2). \tag{3.17}$$

Where we used the pairing rule and because of the symmetries all directions must contribute equally. The second term reads,

$$\frac{\hbar^2}{m_0^2} \sum_{n,i,j} \frac{\langle x | \, p_i \, | n \rangle \langle n | \, p_j \, | x \rangle}{E_v - E_n} k_i k_j = \frac{\hbar^2}{m_0^2} \sum_{n,i} \frac{\langle x | \, p_x \, | n \rangle \langle n | \, p_x \, | x \rangle}{E_v - E_n} k_x^2 = L k_x^2 + M(k_y^2 + k_z^2), \tag{3.18}$$

since the p state x has a chosen direction the term in the x direction can give another contributions then the z and y direction. The third interaction is

$$\frac{\hbar^2}{m_0^2} \sum_{n,i,j} \frac{\langle x | \, p_i \, | n \rangle \langle n | \, p_j \, | y \rangle}{E_v - E_n} k_i k_j = \frac{\hbar^2}{m_0^2} \sum_{n,i} \frac{\langle x | \, p_x \, | n \rangle \langle n | \, p_y \, | y \rangle}{E_v - E_n} k_x k_y + \frac{\hbar^2}{m_0^2} \sum_{n,i} \frac{\langle x | \, p_y \, | n \rangle \langle n | \, p_x \, | y \rangle}{E_v - E_n} k_y k_x = N k_x k_y, \tag{3.19}$$

which follows from the pairing rule. Finally we consider the fourth term:

$$\frac{\hbar^2}{m_0^2} \sum_{n,i,j} \frac{\langle s | \, p_i \, | n \rangle \langle n | \, p_j \, | x \rangle}{\frac{1}{2}(E_c - E_v) - E_n} k_i k_j. \tag{3.20}$$

This term stems from the second order interaction between the conduction band s and the valence bands p. The energy of this interaction is chosen to be $\frac{1}{2}(E_c - E_v)$ as an approximation. First we focus our attention on the term $\langle s | \, p_i \, | n \rangle$. Since all characters of IRR $\Gamma 1$ are 1 it follows from the selection rules that n must be a distant band belonging to the IRR $\Gamma 4$. Now that we have three unpaired basis functions of $\Gamma 4$ its impossible to pair them up. The only way to keep it invariant under C_2 is to have them belong to three different directions, so it will invariant when changing sign of two directions. The full interaction is then given by,

$$\frac{\hbar^2}{m_0^2} \sum_{n,i,j} \frac{\langle s | \, p_i \, | n \rangle \langle n | \, p_j \, | x \rangle}{\frac{1}{2}(E_c - E_v) - E_n} k_i k_j = \frac{\hbar^2}{m_0^2} \frac{\langle s | \, p_y \, | y' \rangle \langle y' | \, p_z \, | x \rangle}{\frac{1}{2}(E_c - E_v) - E_{y'}} k_y k_z + \frac{\hbar^2}{m_0^2} \frac{\langle s | \, p_z \, | z' \rangle \langle z' | \, p_y \, | x \rangle}{\frac{1}{2}(E_c - E_v) - E_n} k_z k_y = B k_y k_z. \tag{3.21}$$

where the two terms contribute equally because of the symmetries. Its worth to notice that this term breaks inversion symmetry since the p orbitals are anti-symmetric. So if our group also contained an inversion symmetry this term would be 0. Because of this the B term is often called the Bulk Inversion asymmetric (BIA) contribution up to second order [11]. The diamond structure is the same structure as zinc blende except that is also contains an inversion symmetry between the two atoms in the structure, so this term is effectively zero in diamond structures [9].

With all interactions considered the second order Hamiltonian is,

$$H_{DKK}\left|\Psi\right\rangle = \begin{bmatrix} A(k_x^2+k_y^2+k_z^2) & Bk_yk_z & Bk_xk_z & Bk_xk_y \\ Bk_yk_z & Lk_x^2+M(k_y^2+k_z^2) & Nk_xk_y & Nk_xk_z \\ Bk_xk_z & Nk_xk_y & Lk_y^2+M(k_x^2+k_z^2) & Nk_yk_z \\ Bk_xk_y & Nk_xk_z & Nk_yk_z & Lk_z^2+M(k_x^2+k_y^2) \end{bmatrix} \begin{bmatrix} s \\ x \\ y \\ z \end{bmatrix}, \tag{3.22}$$

known as the Dresselhouse-Kip-Kittel (DKK) Hamilton. We still know nothing about the value of these terms, but these are often found experimentally or estimated from pseudo-potential methods which we will not engage in. Until now we neglected spin and since our Hamiltonian consists of no terms that break spin symmetry our bands are spin degenerate.

3.2 Spin-Orbit Coupling

The spin-orbit coupling stems form the relativistic effect of the electrons motion around the atoms. In this project, we will be working with zinc blende structures consisting of heavy elements, therefore the atoms have a large electrical field, which will give a significant contribution to the spin-orbit coupling. We will treat this term as a perturbation that lifts the spin degeneracy. A explicit deviation is given in [20]. To low order the spin-orbit coupling is

$$H_{so} = \frac{\hbar}{4m_0^2c^2}(\nabla V \times p)\cdot\sigma = \frac{\hbar}{4m_0^2c^2}(\sigma\times\nabla V)\cdot p, \tag{3.23}$$

So when we apply Bloch states we obtain

$$H_{so}u(k,r) = \left[\frac{\hbar}{4m_0^2c^2}(\sigma\times\nabla V)\cdot(p+\hbar k)\right]u(k,r) \tag{3.24}$$

where we disregarded the k dependent term since the orbital motion of the electrons around the atoms is usually much faster then the group velocity k. Looking at the first form of Eq.3.23, we notice that both ∇V and p transforms as basis vectors for $\Gamma 4$ and there cross product must therefore transform as a axial vector.

The symmetry group of T_d contains a reflection around the plane [1,1,0]. This reflection interchanges the coordinates x and y so for a axial vector which has the form,

$$\nabla V\times p = \epsilon_{\alpha\beta\gamma}\frac{dV}{d\alpha}p_\beta\hat{\gamma} \quad \text{we find the representaion of } \sigma: \quad \begin{pmatrix} 0 & -1 & 0 \\ -1 & 0 & 0 \\ 0 & 0 & -1 \end{pmatrix} \tag{3.25}$$

Where the index span the Cartesian coordinates. This shows that the character for the reflection class must be -1 for axial vectors. These vectors generate a 3 dimensional IRR and it is recognized from table.1 to be $\Gamma 5$.

We now want to obtain selection rules for this perturbation working on our p and s states:

$$\Gamma 5\otimes\Gamma 1 = \Gamma 1 \quad \text{and} \quad \Gamma 5\otimes\Gamma 4 = \Gamma 2\oplus\Gamma 3\oplus\Gamma 4\oplus\Gamma 5 \tag{3.26}$$

From here we se that there is no spin-orbit coupling term between the valence and the conduction band. We will ignore spin orbit terms from distant bands. Since there is only one conduction s state it will be unchanged as it does not couple with the valence bands.

The degenerate valence band couple and this could lift their degeneracy. The coupling between x and y is,

$$\left\langle x\right|\epsilon_{\alpha\beta\gamma}\frac{dV}{d\alpha}p_\beta\left|y\right\rangle\sigma_\gamma = \left\langle x\right|\frac{dV}{dx}p_y - \frac{dV}{dy}p_x\left|y\right\rangle\sigma_z, \tag{3.27}$$

since we have the pairing rule. The pairing rule cannot be met for perturbations between x and x states since they contain isolated y and z terms. We apply symmetries that interchange coordinates and find:

$$\left\langle x\right|\frac{dV}{dx}p_y - \frac{dV}{dy}p_x\left|y\right\rangle = \left\langle y\right|\frac{dV}{dy}p_z - \frac{dV}{dz}p_y\left|z\right\rangle = \left\langle z\right|\frac{dV}{dz}p_x - \frac{dV}{dx}p_z\left|x\right\rangle = \frac{4m_0^2c^2}{3i\hbar}\Delta \tag{3.28}$$

Why this choice of constant is smart will come apparent soon. So the full interaction matrix can be expressed as

$$\sum_{n,m} \langle n| H_{so} |m\rangle = \frac{\Delta}{3i} \begin{bmatrix} 0 & 0 & 0 & 0 \\ 0 & 0 & \sigma_z & -\sigma_y \\ 0 & -\sigma_z & 0 & \sigma_x \\ 0 & \sigma_y & -\sigma_x & 0 \end{bmatrix} \begin{bmatrix} s \\ x \\ y \\ z \end{bmatrix} \tag{3.29}$$

Since a Pauli matrix connects a spin up state with a spin down state, we can write our the full interaction and diagonalize it:

$$\frac{\Delta}{3i} \begin{bmatrix} 0 & 0 & 0 & 0 & 0 & 0 & 0 & 0 \\ 0 & 0 & 0 & 0 & 0 & 0 & 0 & 0 \\ 0 & 0 & 0 & 0 & 1 & 0 & 0 & i \\ 0 & 0 & 0 & 0 & 0 & -1 & -i & 0 \\ 0 & 0 & -1 & 0 & 0 & 0 & 0 & 1 \\ 0 & 0 & 0 & 1 & 0 & 0 & 1 & 0 \\ 0 & 0 & 0 & -i & 0 & -1 & 0 & 0 \\ 0 & 0 & i & 0 & -1 & 0 & 0 & 0 \end{bmatrix} \begin{bmatrix} s\uparrow \\ s\downarrow \\ x\uparrow \\ x\downarrow \\ y\uparrow \\ y\downarrow \\ z\uparrow \\ z\downarrow \end{bmatrix} \rightarrow \frac{\Delta}{3} \begin{bmatrix} 0 & 0 & 0 & 0 & 0 & 0 & 0 & 0 \\ 0 & 0 & 0 & 0 & 0 & 0 & 0 & 0 \\ 0 & 0 & 1 & 0 & 0 & 0 & 0 & 0 \\ 0 & 0 & 0 & 1 & 0 & 0 & 0 & 0 \\ 0 & 0 & 0 & 0 & 1 & 0 & 0 & 0 \\ 0 & 0 & 0 & 0 & 0 & 1 & 0 & 0 \\ 0 & 0 & 0 & 0 & 0 & 0 & -2 & 0 \\ 0 & 0 & 0 & 0 & 0 & 0 & 0 & -2 \end{bmatrix} \begin{bmatrix} \text{Ec}\uparrow \\ \text{Ec}\downarrow \\ \text{Hh}\uparrow \\ \text{Lh}\uparrow \\ \text{Lh}\downarrow \\ \text{Hh}\downarrow \\ \text{Sp}\uparrow \\ \text{Sp}\downarrow \end{bmatrix}. \tag{3.30}$$

Where the arrow indicates a transformation to a diagonal form. Here Ec is the conduction electron, Hh is the heavyhole, Lh is the lighthole and Sp is the split-off hole. Notice that the degeneracy of the valence bands has been lifted. They are now split into two degenerate bands each associated with a spinor room. This can be seen more clearly if we consider the transformation matrix:

$$\begin{bmatrix} \text{Ec}\uparrow \\ \text{Ec}\downarrow \\ \text{Hh}\uparrow \\ \text{Lh}\uparrow \\ \text{Lh}\downarrow \\ \text{Hh}\downarrow \\ \text{Sp}\uparrow \\ \text{Sp}\downarrow \end{bmatrix} = \begin{bmatrix} 1 & 0 & 0 & 0 & 0 & 0 & 0 & 0 \\ 0 & 1 & 0 & 0 & 0 & 0 & 0 & 0 \\ 0 & 0 & \frac{1}{\sqrt{2}} & 0 & \frac{i}{\sqrt{2}} & 0 & 0 & 0 \\ 0 & 0 & 0 & \frac{1}{\sqrt{6}} & 0 & \frac{i}{\sqrt{6}} & -\sqrt{\frac{2}{3}} & 0 \\ 0 & 0 & -\frac{1}{\sqrt{6}} & 0 & \frac{i}{\sqrt{6}} & 0 & 0 & -\sqrt{\frac{2}{3}} \\ 0 & 0 & 0 & -\frac{1}{\sqrt{2}} & 0 & \frac{i}{\sqrt{2}} & 0 & 0 \\ 0 & 0 & 0 & \frac{1}{\sqrt{3}} & 0 & \frac{i}{\sqrt{3}} & \frac{1}{\sqrt{3}} & 0 \\ 0 & 0 & -\frac{1}{\sqrt{3}} & 0 & \frac{i}{\sqrt{3}} & 0 & 0 & \frac{1}{\sqrt{3}} \end{bmatrix} \begin{bmatrix} s\uparrow \\ s\downarrow \\ x\uparrow \\ x\downarrow \\ y\uparrow \\ y\downarrow \\ z\uparrow \\ z\downarrow \end{bmatrix} \tag{3.31}$$

We now show that these states corresponds to states of total angular momentum from spin and movement around the atom. Inspired by atomic physics we define states by their angular momentum [9] as

$$|1,1\rangle = \frac{1}{\sqrt{2}}x + \frac{i}{\sqrt{2}}y, \quad |1,0\rangle = -z, \quad |1,-1\rangle = -\frac{1}{\sqrt{2}}x + \frac{i}{\sqrt{2}}y, \tag{3.32}$$

which we combine with the spin half Hilbert space to obtain the total angular momentum j. There is only one combination that gives a total angular momentum of $j = \frac{3}{2}$,

$$\left|\frac{3}{2},\frac{3}{2}\right\rangle = |1,1\rangle_A \otimes \left|\frac{1}{2},\frac{1}{2}\right\rangle_S \quad \text{and} \quad \left|\frac{3}{2},-\frac{3}{2}\right\rangle = |1,-1\rangle_A \otimes \left|\frac{1}{2},-\frac{1}{2}\right\rangle_S \tag{3.33}$$

so applying the lowering operator on this state we obtain the next state

$$J_{-1}\left|\frac{3}{2},\frac{3}{2}\right\rangle = \sqrt{\frac{3}{2}}\left|\frac{3}{2},\frac{1}{2}\right\rangle = A_{-1}|1,1\rangle_A \otimes \left|\frac{1}{2},\frac{1}{2}\right\rangle_S + |1,1\rangle_A \otimes S_{-1}\left|\frac{1}{2},\frac{1}{2}\right\rangle_S \tag{3.34}$$

$$= |1,0\rangle_A \otimes \left|\frac{1}{2},\frac{1}{2}\right\rangle_S + |1,1\rangle_A \otimes \frac{1}{\sqrt{2}}\left|\frac{1}{2},-\frac{1}{2}\right\rangle_S \Rightarrow \left|\frac{3}{2},\frac{1}{2}\right\rangle = \sqrt{\frac{2}{3}}|1,0\rangle_A\uparrow + \frac{1}{\sqrt{3}}|1,1\rangle_A\downarrow \tag{3.35}$$

Comparing this to our transformation matrix Eq.3.31, we clearly see that our states correspond to

$$\text{Hh}\uparrow = \left|\frac{3}{2},\frac{3}{2}\right\rangle, \quad \text{Lh}\uparrow = \left|\frac{3}{2},\frac{1}{2}\right\rangle, \quad \text{Lh}\downarrow = \left|\frac{3}{2},-\frac{1}{2}\right\rangle, \quad \text{Hh}\downarrow = \left|\frac{3}{2},-\frac{3}{2}\right\rangle \tag{3.36}$$

These states correspond to the four times degenerate spinor space $j = \frac{3}{2}$. The two split-off holes are part of another spinor space. We find these states by noting that it must be a $j = \frac{1}{2}$ space and that its states must be orthogonal to the spinor $\frac{3}{2}$ space. A state in this state is therefore described by

$$\left|\frac{1}{2},\frac{1}{2}\right\rangle = A|1,0\rangle\uparrow + B|1,1\rangle\downarrow \quad \text{and} \quad \left\langle\frac{3}{2},\frac{1}{2}\middle|\frac{1}{2},\frac{1}{2}\right\rangle = 0 \tag{3.37}$$

$$\Rightarrow A\sqrt{\frac{2}{3}} + B\frac{1}{\sqrt{3}} = 0 \Rightarrow \left|\frac{1}{2},\frac{1}{2}\right\rangle = \sqrt{\frac{2}{3}}|1,1\rangle\downarrow - \frac{1}{\sqrt{3}}|1,0\rangle\uparrow \tag{3.38}$$

It follows likewise for the spin down split-off hole. We also recognize these states from the transformation so,

$$\text{Sp}\uparrow = \left|\frac{1}{2},\frac{1}{2}\right\rangle, \quad \text{Sp}\downarrow = \left|\frac{1}{2},-\frac{1}{2}\right\rangle. \tag{3.39}$$

The total angular momentum space is then the space that diagonalizes the spin-orbit interaction.

Our total Hamiltonian is then given by,

$$H = I_{2\times 2}\otimes H_k + I_{2\times 2}\otimes H_{DKK} + H_{so} \tag{3.40}$$

and diagonalizing this matrix according to spin yields our final Hamiltonian. This is done using the transformation matrix Eq.3.31 and we obtain:

$$\begin{bmatrix}
E_c+A_c & 0 & T^*-V^* & \sqrt{2}(W+U) & -\frac{1}{\sqrt{3}}(T+V) & 0 & -(W+U) & \sqrt{\frac{2}{3}}(T-V) \\
0 & E_c+A_c & 0 & \frac{1}{\sqrt{3}}(T^*-V^*) & \sqrt{2}(W^*+U) & -(T+V) & \sqrt{\frac{2}{3}}(T^*-V^*) & W^*+U \\
T-V & 0 & P+Q+E_v & R & S & 0 & \frac{1}{\sqrt{2}}R & \sqrt{2}S \\
\sqrt{2}(W^*+U) & \frac{1}{\sqrt{3}}(T-V) & R^* & P-Q+E_v & 0 & S & -\sqrt{2}Q & \sqrt{\frac{2}{3}}R \\
-\frac{1}{\sqrt{3}}(T^*+V^*) & \sqrt{2}(W+U) & S^* & 0 & P-Q+E_v & -R & -\sqrt{\frac{2}{3}}R^* & \sqrt{2}Q \\
0 & -(T^*+V^*) & 0 & S^* & -R^* & P+Q+E_v & -\sqrt{2}S^* & \frac{1}{\sqrt{2}}R^* \\
-(U+W^*) & \sqrt{\frac{2}{3}}(T-V) & \frac{1}{\sqrt{2}}R^* & -\sqrt{2}Q^* & -\sqrt{\frac{2}{3}}R & -\sqrt{2}S & P+E_v-\Delta & 0 \\
\sqrt{\frac{2}{3}}(T^*-V^*) & W+U & \sqrt{2}S^* & \sqrt{\frac{2}{3}}R^* & \sqrt{2}Q^* & \frac{1}{\sqrt{2}}R & 0 & P+E_v-\Delta
\end{bmatrix}$$

Using the basis:

$$\left[\left|\tfrac{1}{2},\tfrac{1}{2}\right\rangle_c \quad \left|\tfrac{1}{2},-\tfrac{1}{2}\right\rangle_c \quad \left|\tfrac{3}{2},\tfrac{3}{2}\right\rangle_v \quad \left|\tfrac{3}{2},\tfrac{1}{2}\right\rangle_v \quad \left|\tfrac{3}{2},-\tfrac{1}{2}\right\rangle_v \quad \left|\tfrac{3}{2},-\tfrac{3}{2}\right\rangle_v \quad \left|\tfrac{1}{2},\tfrac{1}{2}\right\rangle_v \quad \left|\tfrac{1}{2},-\tfrac{1}{2}\right\rangle_v\right] \tag{3.41}$$

This is the full Luttinger-Kohn Hamilton up to second order in perturbation theory [18]. The definitions of the terms follow here:

$$A_c = (A+\frac{\hbar^2}{2m_0})k^2, \quad P = -\frac{\hbar^2}{2m_0}\gamma_1 k^2, \quad Q = -\frac{\hbar^2}{2m_0}\gamma_2(k_x^2+k_y^2-2k_z^2), \quad R = 2\sqrt{3}\frac{\hbar^2}{2m_0}\gamma_3 k_z k_-,$$
$$S = \sqrt{3}\frac{\hbar^2}{2m_0}\left[\frac{1}{2}(\gamma_3+\gamma_2)k_-^2 - \frac{1}{2}(\gamma_3-\gamma_2)k_+^2\right], \quad T = -\frac{1}{\sqrt{2}}Pk_-, \quad V = \frac{1}{\sqrt{2}}Bk_z k_-, \quad U = \frac{1}{\sqrt{3}}Pk_z,$$
$$W = \frac{i}{\sqrt{3}}Bk_x k_y, \quad k_- = k_x - ik_y, \quad k_+ = k_x + ik_y, \quad E_v = E_v^{kane} - \frac{1}{3}\Delta$$

These terms are expressed in the parameters known as Luttinger parameters since its convention. They can be expressed from the DKK parameters as follows,

$$\gamma_1 = -\frac{2m_0}{3\hbar^2}(L+2M) - 1, \quad \gamma_2 = -\frac{m_0}{3\hbar^2}(L-M), \quad \gamma_3 = -\frac{m_0}{3\hbar^2}N. \tag{3.42}$$

With the final form of the full second order Hamiltonian we are ready to deal with quantum wells which is the topic of the following sections.

4 Heterointerfaces

In order to a achieve a inverted band gap which is one of the characteristics of the topological state, we need to find solutions for quantum wells. A quantum well is a structure consisting of minimum three materials. Our energy bands are located in a host material which is confined by two barrier-materials where the waves decay as they move away from the well. In such a structure only certain k's are allowed because of the finite size of the well. So this effectively reduces the system by one dimension to a two dimensional electron gas (2DEG):

It order to treat such structures properly we need a theory for heterointerfaces, which is the boundary between two different kind of materials. Lets assume that we grow our quantum well along the [0,0,1] direction then k_x and k_y will still be good quantum numbers, but k_z is not. So our Bloch wave functions are no longer a correct description, so we generalize it to,

$$\psi(r) = e^{ik\cdot r}u(k,r) \to \psi(z,r_{||}) = e^{ik_{||}\cdot r_{||}}F(z)u(k,r), \tag{4.1}$$

where $F(z)$ is a slowly varying function in the bulk of the crystal called, the envelope function and $k_{||}$ is a vector in the yz plane. The full solution for the Hamiltonian must consist of a linear combination of such functions. We are only interested in solutions at the Γ point ($k = 0$). So the full wave-function can be expressed as

$$\Psi(z, r_{||}) = \sum_n e^{ik_{||}\cdot r_{||}} F_n(z) u_{n,k=0}(z). \tag{4.2}$$

Where n is the number eigenstates for a given E. The full wave function must be continuous across the whole structure and a often used approximation is to set the zone-center functions u_{n,k_0} equal in all materials and to neglect the behavior of the envelope function at the interface [21]. This leads to continuation of the envelope function at the interface,

$$\Psi^A(z, r_{||}) = \Psi^B(z, r_{||}) \approx \sum_n F_n^A(z_0) = \sum_n F_n^B(z_0). \tag{4.3}$$

from which we obtain n equations where n is the dimension of the Hamiltonian. This approximation is only valid if the structure of the different materials closely resemble one another.

Another set of boundary conditions can be obtained by integration of Schrödinger's equations across the interface. Remembering the origin of the k_z operators we set $k_z \to -i\partial_z$ in our Hamiltonian. Since our materials change across the z direction so does our band parameters, so k_z does not commute with the band parameters. Since our Hamilton is hermitian we need to determine a ordering of these differentials which leads to a hermitian form.

We consider two methods and use the DKK (eqn.3.22) Hamilton as an example. First we consider the standard symmetrization procedure [20]. We order our terms as follows:

$$Ak_z^2 \to k_z A k_z, \quad Pk_z \to \frac{1}{2}(Pk_z + k_z P), \quad Nk_z k_x \to \frac{1}{2}(k_z N k_x + k_x N k_z). \tag{4.4}$$

This method achieves a hermitian form but is not the only way of doing this. The arbitrariness of the symmetrization lead many to believe it was wrong. Instead Burt developed a method for obtaining the correct ordering of terms by developing a wave-function, with artificial zone-center functions that are similar in all materials of the heterostructure [3].

He found that the ordering of k's is determined from its origin in perturbation. If we consider second order Lowdin perturbation, the ordering is found to be

$$\frac{\hbar^2}{m_0^2} \sum_{n,i,j} \frac{\langle x| p_i |n\rangle \langle n| p_j |y\rangle}{E_v - E_n} k_i k_j \to k_i \frac{\hbar^2}{m_0^2} \sum_{n,i,j} \frac{\langle x| p_i |n\rangle \langle n| p_j |y\rangle}{E_v - E_n} k_j \tag{4.5}$$

This obtains the same result as symmetrization when $i = j$. But for off diagonal B and N terms ordering will change. The ordering of B is easy, since their is only contributions from one band (Eq.3.21). The ordering of N can be found if you neglect contributions from the $\Gamma 5$ bands. This was done by Foreman in [4]. For $H_{X,Y}^{DKK}$ he found the terms,

$$H_{X,Y}^{DKK} = Nk_x k_y \Rightarrow k_x N_+ k_y + k_y N_- k_x \quad \text{where} \quad N_- = M, \quad N_+ = N - N_-. \tag{4.6}$$

with $H_{X,Y}^{DKK}$ describing the interaction between the x valence and the y valence band. Both these methods reduces to the bulk Hamiltonian when k_z commutes with band parameters which is true far from the interface. We are finally able to integrate the Schrödinger equation across the interface. To show how we consider the following example:

$$\sum_n \left[-\partial_z A \partial_z F_{n,c}(z) - \sum_j i\partial_z B k_x F_{n,j}(z) - \sum_j i k_x C \partial_z F_{n,j}(z) \right] = E \sum_n F_{n,c}(z). \tag{4.7}$$

Where the interface is considered to abrupt so our band parameters change as deltafunctions. By integration over a infinitesimal length across the interface all terms that are not deltafunctions will go to zero. Which leaves,

$$\sum_n \left[A^A \partial_z F_{n,c}^A - i \sum_j B^A k_x F_{n,j}^A \right] - \sum_n \left[A^B \partial_z F_{n,c}^B - i \sum_j B^B k_x F_{n,j}^B \right] = 0. \tag{4.8}$$

from this we obtain n more boundary conditions, so we now in total have $2n$ boundary conditions at each interface. Now treating the DKK hamiltonian (Eq.3.22) by using Eq.4.8 we find a current operator for both Burt's ordering

and symmetrization:

$$J_B = \begin{pmatrix} A\partial_z & i\frac{B}{2}k_y & i\frac{B}{2}k_x & 0 \\ i\frac{B}{2}k_y & M\partial_z & 0 & iN_-k_x \\ i\frac{B}{2}k_x & 0 & M\partial_z & iN_-k_y \\ 0 & iN_+k_x & iN_+k_y & L\partial_z \end{pmatrix}, \quad J_S = \begin{pmatrix} A\partial_z & i\frac{B}{2}k_y & \frac{B}{2}k_x & 0 \\ i\frac{B}{2}k_y & M\partial_z & 0 & i\frac{N}{2}k_x \\ i\frac{B}{2}k_x & 0 & M\partial_z & i\frac{N}{2}k_y \\ 0 & i\frac{N}{2}k_x & i\frac{N}{2}k_y & L\partial_z \end{pmatrix}. \tag{4.9}$$

Here we notice that the old symmetrization method produces a symmetric current operator while Burt's method produces a non-symmetric. It has been found that Burt's J_B, derived from first-hand calculations produce better results then J_S, where symmetrization is just assumed to obtain a symmetric current operator [17].

Now that we have our boundary conditions we can chose a trial function for the envelope function,

$$F = e^{ik_z z}\begin{pmatrix} f_1 \\ \vdots \\ f_n \end{pmatrix} \quad \text{with } k_z \text{ given by} \quad |H(k_z) - E| = 0 \tag{4.10}$$

This determinant gives an n order polynomial for k_z^2 which in total gives $2n$ envelope functions in each material. Since we have $m-1$ interfaces, where m is the number of materials, we have enough boundary conditions to determine the envelope function if the in- and out-going waves are set to zero. We will now use this theory to obtain 2DEGs.

5 HgTe inverted band model

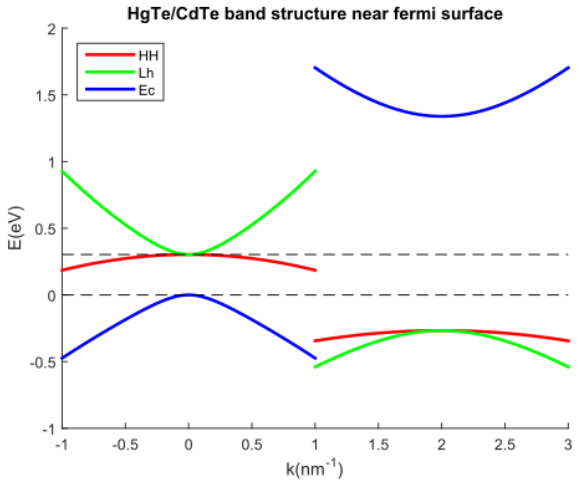

Figure 1: Dispersion near the fermi energy. HgTe to the left. CdTe to the right.

The zinc blende structure HgTe is characterized by a inverted band gap [13]. This inverted gap is partly due to the large spin-orbit interaction which pushes the valence band up by $\Delta/3$. The inverted band is a prerequisite for a topological state, but HgTe is not by itself a topological insulator, since the Fermi energy is placed at the degenerate intersection between the Lh and the Hh band. The topological phase requires a band gap to obtain isolated edge states. In order to make this into a topological insulator we need to separate the Lh from the Hh states. This can be done in a quantum well where finite size will separate bands of different curvature. The HgTe layer will be placed between 2 layers of CdTe which will act as outer barriers.

We are looking for a region where the first Ec state have lower energy then the first Hl state. Here the Hl will be behaving as a standing wave and the Ec as a localized state at the CdTe edges.

Following the method of [2] we begin by finding ground-states in each material by assuming the crystal is grown in the z direction and setting $k_x = k_y = 0$. These states will then be treated as a basis for perturbation around $k_x, k_y \neq 0$ from which we derive an effective model for the electron-heavyhole interaction.

In our Hamiltonian we ignore the Bulk Inversion Asymmetric (BIA) term B, since this is very small in HgTe structures [13]. Our quantum well is also structural symmetric since the barriers on each side of the well are identical.

In the $k_x = k_y = 0$ direction our Hamiltonian Eq.3.41 separates into a spin-up and a spin-down part. Consider the spin up,

$$H_\uparrow(0,0,-i\frac{\partial}{\partial z})\Psi(z) = \begin{pmatrix} E_c - \partial_z A_c \partial_z & -i\sqrt{\frac{2}{3}}P\partial_z & \frac{i}{\sqrt{3}}P\partial_z & 0 \\ -i\sqrt{\frac{2}{3}}P\partial_z & E_v - \partial_z h_l \partial_z & \sqrt{2}Q & 0 \\ \frac{i}{\sqrt{3}}P\partial_z & \sqrt{2}Q & E_v - \Delta - \partial_z h_{sp}\partial_z & 0 \\ 0 & 0 & 0 & E_v - \partial_z h_h \partial_z \end{pmatrix} \begin{pmatrix} \left|\frac{1}{2},\frac{1}{2}\right\rangle_c \\ \left|\frac{3}{2},\frac{1}{2}\right\rangle_v \\ \left|\frac{1}{2},\frac{1}{2}\right\rangle_v \\ \left|\frac{3}{2},\frac{3}{2}\right\rangle_v \end{pmatrix}. \tag{5.1}$$

We clearly see that the Hh decouple from the rest of the bands, so we solve it separately. We will treat the split-off hole as a distant band since its placed far from the region of interest due to the large spin-orbit coupling [2]. We will correct the conduction band energy using perturbation theory. So we need to modify our band parameters as follows,

$$A_C = A_c + \frac{1}{3}\frac{P^2}{E_c - E_v + \Delta}, \quad h_l = \frac{\hbar^2}{2m_0}(\gamma_1 + 2\gamma_2), \quad h_h = \frac{\hbar^2}{2m_0}(\gamma_1 - 2\gamma_2). \tag{5.2}$$

where we have taken our band parameters from [13].

We start by solving the Ec-Lh envelope, we know that both of these states are decaying in the region between the valence and conduction band. We choose the trial function

$$\Psi_{ec-ll} = e^{\lambda z}\begin{pmatrix} f \\ g \end{pmatrix}, \tag{5.3}$$

and insert it into our Hamiltonian

$$\begin{vmatrix} E_c - A_C\lambda^2 - E & -i\sqrt{\frac{2}{3}}P\lambda \\ -i\sqrt{\frac{2}{3}}P\lambda & E_v + h_l\lambda^2 - E \end{vmatrix} = 0 \tag{5.4}$$

and shift notation to,

$$C = \frac{E_c + E_v}{2}, \quad A = \frac{E_c - E_v}{2}, \quad D = \frac{A_C + h_l}{2}, \quad B = \frac{A_C - h_l}{2}, \quad E_C = E - C \tag{5.5}$$

so by solving for λ^2 we get

$$\lambda^2_{+,-=1,2} = F \pm \sqrt{F^2 - \frac{A^2 - E_C^2}{G}} \quad \text{with} \quad G = B^2 - D^2 \quad \text{and} \quad F = \frac{\frac{2}{3}P^2 + 2(AB + E_C D)}{G}. \tag{5.6}$$

From this we obtain 4 λ, labeled 1 and 2 which satisfy the equations. For the given material parameters F is positive and $F^2 > \frac{A^2 - E_C^2}{G}$. By Eq.5.6 we see that our solutions are either completely imaginary or completely real. From numerical calculations within the region of interest we find that λ_1 is always real and much larger then λ_2. These large λ_1 values behaves unphysical and we classify them as spurious solution. Spurious solutions are a common problem in $k \cdot p$ theory and arise from the non-parabolic terms of high order, like $A_C h_l \lambda^4$. Different methods for treating them is discussed by several authors [16][17] but no general way of eliminating them has been found. In the next section we will present a method for removing them when $A_C \approx 0$ but this is not the case for HgTe. It has been shown that effective models for quantum wells can be obtained simply by removing all spurious solutions [16].

We now consider the eigenvectors which are determined by:

$$\begin{pmatrix} A + (D+B)\lambda^2 - E_C & -i\sqrt{\frac{2}{3}}P\lambda \\ -i\sqrt{\frac{2}{3}}P\lambda & -A + (D-B)\lambda^2 - E_C \end{pmatrix}\begin{pmatrix} f \\ g \end{pmatrix} = 0, \quad \begin{pmatrix} f(\lambda) \\ g(\lambda) \end{pmatrix} = \begin{pmatrix} -A + (D-B)\lambda^2 - E_C \\ i\sqrt{\frac{2}{3}}P\lambda \end{pmatrix} \tag{5.7}$$

This eigenvector is correct since it reduces the matrix to the determinant equation. Notice that the top part of the eigenvector is symmetric in γ while the bottom part is antisymmetric in γ. We label our constants according to the material they are in as A^{hg} or A^{cd}. Following standard procedure we set ingoing terms in the barrier material equal to zero, since we are looking for confined states. Also to utilize the symmetry of the well we will be describing our wave functions in terms of hyperbolic functions.

So in the three region the waves are

$$(a+b)e^{\lambda^{cd}z}\begin{pmatrix} f(\lambda) \\ g(\lambda) \end{pmatrix}^{cd} \quad \text{(I)} \quad c\begin{pmatrix} f(\lambda)\cosh(\lambda z) \\ g(\lambda)\sinh(\lambda z) \end{pmatrix}^{hg} + d\begin{pmatrix} f(\lambda)\sinh(\lambda z) \\ g(\lambda)\cosh(\lambda z) \end{pmatrix}^{hg} \quad \text{(II)} \quad (a-b)e^{-\lambda^{cd}z}\begin{pmatrix} f(\lambda) \\ -g(\lambda) \end{pmatrix}^{cd} \quad \text{(III)} \tag{5.8}$$

The symmetric and the anti-symmetric part will be solved separately. They split into two systems

$$ae^{\lambda^{cd}z}\begin{pmatrix} f(\lambda) \\ g(\lambda) \end{pmatrix}^{cd} \quad \text{(I)} \quad c\begin{pmatrix} f(\lambda)\cosh(\lambda z) \\ g(\lambda)\sinh(\lambda z) \end{pmatrix}^{hg} \quad \text{(II)} \quad ae^{-\lambda^{cd}z}\begin{pmatrix} f(\lambda) \\ -g(\lambda) \end{pmatrix}^{cd} \quad \text{(III)} \tag{5.9}$$

$$be^{\lambda^{cd}z}\begin{pmatrix} f(\lambda) \\ g(\lambda) \end{pmatrix}^{cd} \quad \text{(I)} \quad d\begin{pmatrix} f(\lambda)\sinh(\lambda z) \\ g(\lambda)\cosh(\lambda z) \end{pmatrix}^{hg} \quad \text{(II)} \quad be^{-\lambda^{cd}z}\begin{pmatrix} -f(\lambda) \\ g(\lambda) \end{pmatrix}^{cd} \quad \text{(III)} \tag{5.10}$$

In this problem our set of linear equations are overdetermined since we have 12 boundary conditions and only 6 coefficients after removing the spurious solutions. Following the calculations of [2] we ignore continuation of

probability current and only use continuation of envelope functions. We eliminate the parameters a,c and d in each equation to obtain a transcendent equation for λ for each symmetry and obtain

$$\text{Ec-sym Eq.5.9} \quad \frac{f(\lambda)^{hg}g(\lambda)^{cd}}{f(\lambda)^{cd}g(\lambda)^{hg}} = -\coth\left(\lambda^{hg}d\right) \quad \text{Lh-sym Eq.5.10} \quad \frac{f(\lambda)^{hg}g(\lambda)^{cd}}{f(\lambda)^{cd}g(\lambda)^{hg}} = -\tanh\left(\lambda^{hg}d\right) \tag{5.11}$$

Here d is two times the length of the well. By using Eq.5.6 to determine λ we obtain two transcendent equations for energy. Using these equations we can for a given length of the well, find the energies for the Ec and Lh band numerically.

The Hh is more simple to solve. From Eq.6.1 and using the same trial solution we have the expression

$$\mu = \pm\sqrt{\frac{E_v - E}{h_h}} \tag{5.12}$$

Where μ is k_z. We split this into a symmetric and a antisymmetric equation. Since we the first Hh state is symmetric we only consider the envelopes

$$ae^{-\mu^{cd}z} \quad \text{(I)} \quad b\cosh\left(\mu^{hg}z\right) \quad \text{(II)} \quad ae^{\mu^{cd}z} \quad \text{(III)} \tag{5.13}$$

For a one band model the probability current reduces to

$$h_h^{cd}\frac{\partial\psi^{cd}}{\partial z} = h_h^{hg}\frac{\partial\psi^{hg}}{\partial z} \quad \text{and we obtain:} \quad \frac{h_h^{hg}\mu^{cd}}{h_h^{cd}\mu^{hg}} = -\tanh\left(\mu^{hg}d\right) \tag{5.14}$$

We are able now to find the states numerically. We want to find at what length of the well will the first Ec band cross the first Hh band. We solve this numerically by iterating over different quantum well lengths and we obtain a crossing at $L_c = 6.73$nm. If $L > L_c$ we obtain an inverted band where the Hh band acts as a conduction band

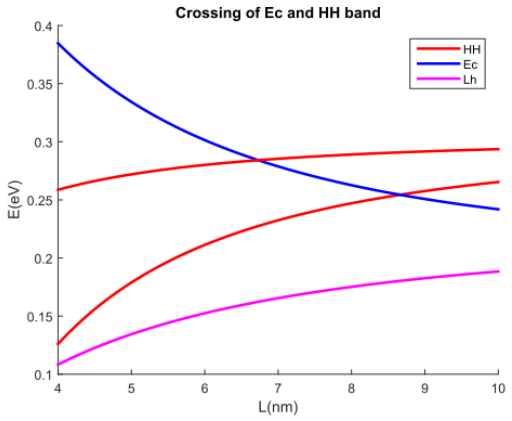

(a) Energy of bands at different quantum well lengths. Crossing of HH and Ec band happens at $L_c \approx 6.73nm$. The crossing of the Ec band with the second HH band happen at $L \approx 8.66nm$

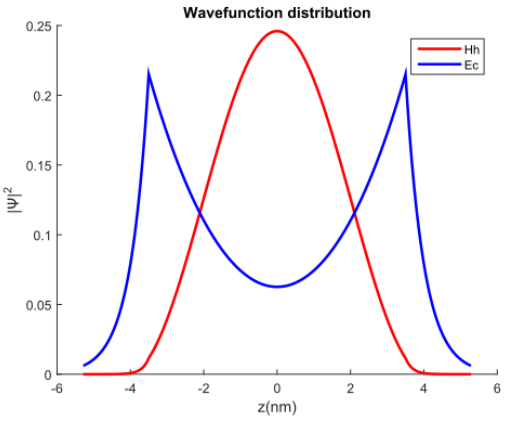

(b) The distribution of the envelope functions in the quantum well at $k_x = k_y = 0$ and L=7nn

Figure 2: Numerical results of HgTe well

and the Ec band acts as a hole band. At $L \approx 8.66$nm the Ec band crosses the second Hh band and the system enters a normal insulating state where the Fermi energy is placed between two Hh states.

5.1 The BHZ hamiltonain

Now that we have the crossing we want to find a effective Hamiltonian for the Hh and the Ec state close to the crossing, where all other bands can be ignored. This is done by perturbation theory. First we normalize the envelope function across the well, which is split into the 3 regions. We show these calculations for the Hh state

$$1 = \int_{-\infty}^{\infty} dz\Psi^*\Psi \Rightarrow 1 = a_h^2\left[\int_{-\infty}^{-d} dze^{2\mu^{cd}z} + \int_{-d}^{d} dz\frac{\cosh\left(\mu^{hg}z\right)^2}{\cosh(\mu^{hg}d)^2}e^{-2\mu^{cd}d} + \int_{d}^{\infty} dze^{-2\mu^{cd}z}\right]$$

$$a_h = e^{\mu^{cd}d}\left[\frac{1}{\mu^{cd}} + \frac{\tanh\left(\mu^{hg}d\right)}{\mu^{hg}} + \frac{d}{\cosh(\mu^{hg}d)^2}\right]^{-1}. \tag{5.15}$$

$L(nm)$	$C(eV)$	$M(eV)$	$D(eV\cdot nm^2)$	$B(eV\cdot nm^2)$	$A(Ev\cdot nm)$
7	0.282	-0.0033	0.0278	-0.147	-0.383
6	0.291	0.0107	0.0207	-0.154	-0.408

Table 2: Parameters for the BHZ Hamiltonian

For the electron state we obtain

$$a_e = e^{\lambda^{cd}d}\left[\frac{(f^{cd})^2+(g^{cd})^2}{\lambda^{cd}} + (f^{hg})^2\frac{\tanh(\mu^{hg}d)}{\lambda^{hg}} + (g^{hg})^2\frac{\coth(\lambda^{hg}d)}{\lambda^{hg}} + \frac{d(f^{hg})^2}{\cosh(\lambda^{hg}d)^2} - \frac{d(g^{hg})^2}{\sinh(\lambda^{hg}d)^2}\right]^{-1}. \quad (5.16)$$

For spin-down we obtain precisely the same. Now we will use perturbation around $k_x, k_y \neq 0$ using the spin-up and spin-down Ec and Hh state as our basis.

$$H^{eff}_{n,m}(k_x,k_y) = \int_{-\infty}^{\infty} dz\, \langle\Psi_n|\, H(k_x,k_y)_{6\times6}\, |\Psi_m\rangle \quad (5.17)$$

Here $H(k_x,k_y)_{6\times6}$ is the same matrix as Eq.3.41 with $B=0$ and removing the two split-off states. First we find the zero couplings. Listed here are the zero coupling arising from their interaction matrix elements being 0:
1. Hh↑ Hh↓ 2. Lh↑ Lh↓ 3. Ec↑ Ec↓ 4. Ec↑ Hh↓

So now there are only two couplings between spin-up and spin-down. The Lh↑-Ec↓ coupling and the Hh↑ $-Lh\downarrow$ coupling. But since Hh and Ec is symmetric with respect to z, and Lh is anti-symmetric in z the integrals vanishes. So there is no coupling between spin-up and spin-down states. If the quantum well was asymmetric we could not guarantee that the wavefunctions would be symmetric/antisymmetric so this would generate a coupling between the spin up and spin down states. As a example consider the integral

$$H^{eff}_{hh,hh}(k_x,k_y) = \int_{-\infty}^{\infty} dz\, \langle\Psi_{hh}|\, H(k_x,k_y)_{6\times6}\, |\Psi_{hh}\rangle \quad (5.18)$$

$$= \int_{-\infty}^{-d} dz\, \left\langle\Psi^{cd}_{hh}\right|\, H^{cd}(k_x,k_y)_{6\times6}\, \left|\Psi^{cd}_{hh}\right\rangle + \int_{-d}^{d} dz\, \left\langle\Psi^{hg}_{hh}\right|\, H^{hg}(k_x,k_y)_{6\times6}\, \left|\Psi^{hg}_{hh}\right\rangle + \int_{d}^{\infty} dz\, \left\langle\Psi^{cd}_{hh}\right|\, H^{cd}(k_x,k_y)_{6\times6}\, \left|\Psi^{cd}_{hh}\right\rangle \quad (5.19)$$

$$= a_h^2 e^{-2\mu^{cd}d}\left[\frac{h_h^{cd}(k_x,k_y)}{\mu^{cd}} + h_h^{hg}(k_x,k_y)\frac{\tanh(\mu^{hg}d)}{\mu^{hg}} + h_h^{cd}(k_x,k_y)\frac{d}{\cosh(\mu^{hg}d)^2}\right]. \quad (5.20)$$

Then evaluating the off-diagonal element

$$\int_{-\infty}^{\infty} dz\, \langle\Psi_{hh}|\, H(k_x,k_y)_{6\times6}\, |\Psi_{ec}\rangle = \int_{-\infty}^{\infty} dz\, \langle\psi_{hh}|\, -\frac{1}{\sqrt{2}}Pk_-\, |\psi_{ec}\rangle + \int_{-\infty}^{\infty} dz\, \langle\psi_{hh}|\, R\, |\psi_{hl}\rangle\,, \quad (5.21)$$

Where the definition of the R term is

$$R = -\frac{\hbar^2}{2m_0}\sqrt{3}k_-\,\{\gamma_3, -i\partial_z\} \quad \text{and} \quad \partial_z\gamma_3 = \gamma_3^{cd}(\delta(z+d)+\delta(z-d)) + \gamma_3^{hg}(\delta(z+d)-\delta(z-d)), \quad (5.22)$$

and the derivatives of band parameters are delta functions, since they change as heavy-sides: It should be stated that in our calculations we have neglected the κ term also given with the material parameters [13]. This term is due to the asymmetric ordering of the N term from Burt's theory, which at the heterointerface also produces a coupling of Lh↑ and Lh↓ due to the asymmetry of the interface. In our deviation of Eq.3.41 these terms are not present since we have not started from Burt's envelope function approach. We use a symmetric ordering which changes $\gamma \to \gamma_3$. These delta functions can then be evaluated by integration. After all these calculations we obtain the effective Hamiltonian for the Ec-Hh coupling,

$$H_{BHZ} = \begin{pmatrix} C+M-(D+B)k_{||}^2 & Ak_- & 0 & 0 \\ Ak_+ & C-M-(D-B)k_{||}^2 & 0 & 0 \\ 0 & 0 & C+M-(D+B)k_{||}^2 & -Ak_+ \\ 0 & 0 & -Ak_- & C-M-(D-B)k_{||}^2 \end{pmatrix} \quad (5.23)$$

In tabel.2 we present the parameters for two different lengths. The first is in the inverted regime and the second is in the normal regime. This model is known as the Bernevig-Hughes-Zhang (BHZ) model and is one of the

simplest models for a topological insulator. In the calculations of [2] a crossing at 6.4nm was found, which is close to what we obtain.

It is important to notice that the hybrid states of the BHZ model can still be labeled according to their symmetry. The electron/light-hole transform as s orbital ($\Gamma 1$) since the electron has always been symmetric and the Lh anti-symmetry is fixed by the anti-symmetry of its envelope function. While the Hh is still anti-symmetric.

6 InAs/GaSb broken band gap model

It was proposed that the InAsGaSb quantum well could have a topological insulating regime [5]. In this section we will try to verify this prediction by finding where the crossing into the topological regime occurs and develop a effective Hamiltonian describing the band interactions close to this crossing. None of the materials of this well have a inverted gap. The unique feature of the InAsGaSb well is the broken band gap where the conduction band InAs has lower energy then the valence band of GaSb.

AlAs is simply a barrier material with a giant gap between its valence and conduction band so we obtain decaying solutions in this material. We will search for bound states in the region between the bottom of the

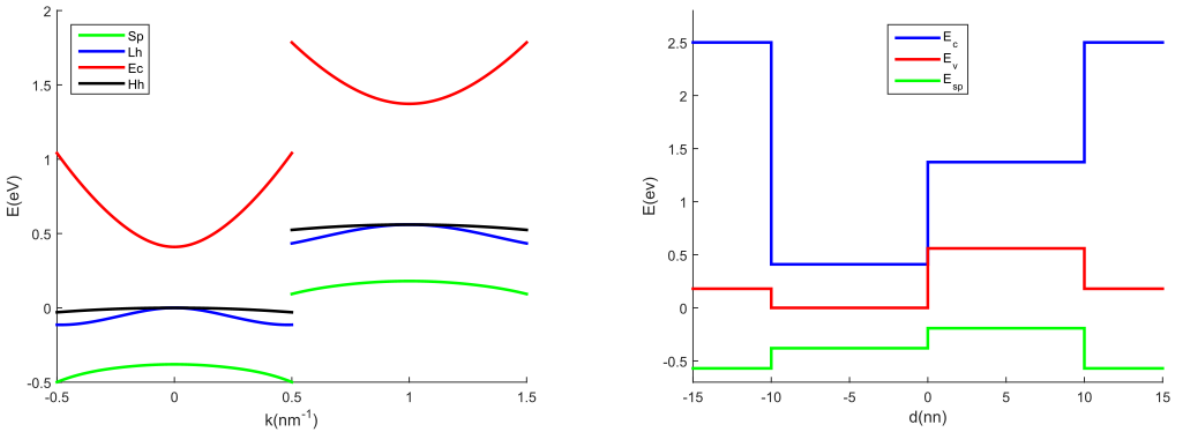

(a) Band structure of InAs and GaSb. InAs to the left, and GaSb to the right.

(b) The energy levels across the quantum well. The two ends are the barrier material AlSb.

Figure 3: The InAsGaSb quantum well

conduction band of InAs and the top of the valence band of GaSb. Much of this project has been dedicated to developing a model for this system, but many complication makes this analytically simple task quite bothersome. The two main problems are:

- Numerical instability from evanescent waves.
- Spurious solutions from high order polynomials in k_z.

The problem of numerical instability makes any calculation difficult but can be reduced by use of scattering matrices [14].

6.1 Forman method

In a famous article Foreman discovered a method to remove some of the spurious solutions for heterostructures, when the distant bands contribution to the conduction band almost cancel out the electron mass [4]. As in HgTe we want to solve for a crystal structure grown in the z direction and we treat k_x and k_y as a perturbation to this model. The spin-up and spin-down direction split into 2 blocks and the heavy-hole decouple from the rest of the bands, so we have the Hamiltonian

$$H_\uparrow(0,0,-i\frac{\partial}{\partial z})\Psi(z) = \begin{pmatrix} E_c - \partial_z A_c \partial_z & -i\sqrt{\frac{2}{3}}P\partial_z & \frac{i}{\sqrt{3}}P\partial_z \\ -i\sqrt{\frac{2}{3}}P\partial_z & E_v - \partial_z h_l \partial_z & -\sqrt{2}\partial_z q \partial_z \\ \frac{i}{\sqrt{3}}P\partial_z & -\sqrt{2}\partial_z q\partial_z & E_v - \Delta - \partial_z h_{sp}\partial_z \end{pmatrix} \begin{pmatrix} \left|\frac{1}{2},\frac{1}{2}\right\rangle_c \\ \left|\frac{3}{2},\frac{1}{2}\right\rangle_v \\ \left|\frac{1}{2},\frac{1}{2}\right\rangle_v \end{pmatrix} \tag{6.1}$$

$$q = \frac{\hbar^2}{2m_0}\gamma_2, \quad h_l = \frac{\hbar^2}{2m_0}(\gamma_1 + 2\gamma_2), \quad h_h = \frac{\hbar^2}{2m_0}(\gamma_1 - 2\gamma_2). \tag{6.2}$$

Where A_c is given in terms of the effective mass of the electrons. We take our material parameters from [12]. Since the parameters are measured as effective mass's where other bands are only considered as perturbations, we need to modify our parameters since we consider these bands explicitly. [4]

$$\gamma_1 = \gamma_{1,m} - \frac{E_P}{3E_g}, \quad \gamma_2 = \gamma_{2,m} - \frac{E_P}{6E_g}, \quad \gamma_3 = \gamma_{3,m} - \frac{E_P}{6E_g}, \quad E_P = \frac{2m_0P^2}{\hbar^2} \tag{6.3}$$

$$A_c = \frac{\hbar^2}{2m_c} - \frac{2P^2}{3E_g} - \frac{P^2}{3(E_g+\Delta)}. \tag{6.4}$$

Here E_g is the gap between the valence bands and the electron band. In these materials A_c is small, so solving the Hamiltonian for k_z will lead to 6.order polynomial and since A_C is small spurious solutions of a very high k_z will be present. Foreman proposed to set $A_c = 0$ thereby making a flatband model for Ec. Following his procedure we eliminate A_c by modifying P. We set $A_C = 0$ and solve Eq.6.4 for P^2:

$$P^2 = \frac{\hbar^2}{2m_c}\left[\frac{2}{3E_g} + \frac{1}{3(E_g+\Delta)}\right]^{-1} \tag{6.5}$$

Now we can generate a table comparing the modified P with the P from [12]. The only material where this

$E_p = \frac{\hbar^2}{2m_0}P^2$	InAs	GaSb	AlSb
eqn.6.5	$20.3eV$	$23.0eV$	$14.0eV$
[12]	$22.2eV$	$22.4eV$	$18.8eV$
Comparison	9.11%	2.80%	33.3%

Table 3: Comparison of different P

approximation is bad is in AlSb. This is not problematic since AlSb is only a barrier material and changes of A_c will only alter the decay rate, which only modifies the band structure a little.

So we set $A_c = 0$. Now we have reduced our polynomial for k_z to fourth order. Using the continuation of the envelope function and probability current we have in total 18 boundary equations. We only have 12 k_z when the ingoing waves are set to zero, so at the moment our system is overdetermined.

When $A_c = 0$ we can express the Ec band as

$$f_1 = \frac{1}{E - E_c}\left(\sqrt{\frac{2}{3}}Pk_zf_2 - \frac{1}{\sqrt{3}}Pk_zf_3\right) \tag{6.6}$$

The Ec envelope then plays a passive role since its completely determined by the holes and will be eliminated from the Hamiltonian. by inserting Eq.6.6 into our Hamiltonian we find:

$$H = \begin{pmatrix} E_v + H_lk_z^2 & Qk_z^2 \\ Qk_z^2 & E_v - \Delta + H_{sp}k_z^2 \end{pmatrix} \tag{6.7}$$

$$H_l = h_l + \frac{2}{3}\frac{P^2}{E - E_c}, \quad H_{sp} = h_{sp} + \frac{1}{3}\frac{P^2}{E - E_c}, \quad Q = \sqrt{2}q + \frac{2}{3}\frac{P^2}{E - E_c} \tag{6.8}$$

In the theory for heterostructures developed by Burt the Kane matrix element P was set to the same value in all materials which leaves the ordering of the term insignificant. Since we have broken this assumption the ordering is no longer trivial. In order to find a self-consistent Hamiltonian we need to eliminate 3 equations from the probability current. This can be done by choosing the ordering,

$$H_{12} = -i\sqrt{\frac{2}{3}}P\partial_z, \quad H_{21} = -i\sqrt{\frac{2}{3}}\partial_z P, \tag{6.9}$$

and by integration we obtain the probability current,

$$J = \begin{pmatrix} A_ck_z & 0 & 0 \\ \sqrt{\frac{2}{3}}P & h_lk_z & \sqrt{2}qk_z \\ \frac{1}{\sqrt{3}}P & \sqrt{2}qk_z & h_{sp}k_z \end{pmatrix} \quad \text{let } A_c = 0 \quad \rightarrow \quad J = \begin{pmatrix} H_lk_z & Q_1k_z \\ Q_2k_z & H_{sp}k_z \end{pmatrix}, \tag{6.10}$$

so we end with 12 coefficients and 12 equations, which is self-consistent. Foreman assumed this ordering to be the correct even though it is not derived, since it keeps the system self-consistent [4].

6.2 Scattering matrices

Inspired by the work of [6], we use scattering matrices to obtain the band structure of this well. We will here present a review of the work which lead to the necessity of the method and show how one uses scattering matrices to obtain solutions for a quantum well. Using the same method as in calculations of HgTe we find the polynomial equations for k_z and eigenvectors to be,

$$k_z^2 = F \pm \sqrt{F^2 - \frac{E_C^2 - A^2}{G}}, \quad \mathbf{f_j^+} = \mathbf{f_j^-} = \begin{pmatrix} -A + (D-B)k_{z,j}^2 - E_C \\ Qk_{z,j}^2 \end{pmatrix} \tag{6.11}$$

$$G = D^2 - B^2 - Q^2, \quad F = \frac{AB + E_C D}{G}, \tag{6.12}$$

$$E_C = E - C, \quad C = \frac{E_v + E_v - \Delta}{2}, \quad A = \frac{E_v - E_v + \Delta}{2}, \quad D = \frac{H_l + H_{sp}}{2}, \quad B = \frac{H_l - H_{sp}}{2}. \tag{6.13}$$

We express our envelope function as

$$\mathbf{\Psi_n} = \sum_j a_{j,n}\mathbf{f_{j,n}^+}e^{ik_{j,n}(z-d_{n-1})} + b_{j,n}\mathbf{f_{j,n}^-}e^{-ik_{j,n}(z-d_n)} \tag{6.14}$$

Where d_n is the coordinate for the right interface, while d_{n-1} is for the left interface and n label different materials. This wave gives a better normalization since it considers where each wave if starting from.

Consider an interface between material n and $n+1$ then we have the boundary conditions

$$\begin{pmatrix} \mathbf{f_n^+} & \mathbf{f_n^-} \\ \mathbf{J_n^+} & \mathbf{J_n^-} \end{pmatrix} \begin{pmatrix} \mathbf{D_n} & 0 \\ 0 & 1 \end{pmatrix} \begin{pmatrix} \mathbf{a_n} \\ \mathbf{b_n} \end{pmatrix} = \begin{pmatrix} \mathbf{f_{n+1}^+} & \mathbf{f_{n+1}^-} \\ \mathbf{J_{n+1}^+} & \mathbf{J_{n+1}^-} \end{pmatrix} \begin{pmatrix} 1 & 0 \\ 0 & \mathbf{D_{n+1}} \end{pmatrix} \begin{pmatrix} \mathbf{a_{n+1}} \\ \mathbf{b_{n+1}} \end{pmatrix} \tag{6.15}$$

$$\mathbf{f_n^+} = (\mathbf{f_{n,1}^+}, \cdots, \mathbf{f_{n,j}^+}), \quad \mathbf{J_n^+} = (\mathbf{J_{n,1}^+}\mathbf{f_{n,1}^+}, \cdots, \mathbf{J_{n,j}^+}\mathbf{f_{n,j}^+}) \tag{6.16}$$

Where $\mathbf{D_n}$ is a diagonal matrix describing the distance traveled by each wave to reach the interface. Its components are

$$D_{n,j,j} = e^{ik_{j,n}(d_n - d_{n-1})} \tag{6.17}$$

We define the transfer matrix as

$$\begin{pmatrix} \mathbf{a_n} \\ \mathbf{b_n} \end{pmatrix} = \mathbf{T}(n, n+1) \begin{pmatrix} \mathbf{a_{n+1}} \\ \mathbf{b_{n+1}} \end{pmatrix} \quad \rightarrow \quad \mathbf{T}(n, n+1) = \begin{pmatrix} \mathbf{D_n^{-1}} & 0 \\ 0 & 1 \end{pmatrix} \begin{pmatrix} \mathbf{f_n^+} & \mathbf{f_n^-} \\ \mathbf{J_n^+} & \mathbf{J_n^-} \end{pmatrix}^{-1} \begin{pmatrix} \mathbf{f_{n+1}^+} & \mathbf{f_{n+1}^-} \\ \mathbf{J_{n+1}^+} & \mathbf{J_{n+1}^-} \end{pmatrix} \begin{pmatrix} 1 & 0 \\ 0 & \mathbf{D_{n+1}} \end{pmatrix} \tag{6.18}$$

These transfer matrices are 4.dimensional. With this formalism we are now able to construct a transfer matrices from one end of the well to the other and by multiplying them together we obtain:

$$\begin{pmatrix} \mathbf{a_0} \\ \mathbf{b_0} \end{pmatrix} = \mathbf{T}(0, N) \begin{pmatrix} \mathbf{a_N} \\ \mathbf{b_N} \end{pmatrix}. \tag{6.19}$$

Since we are looking for bound states we set $\mathbf{b_0} = \mathbf{a_N} = 0$. Then we obtain a solution for our bands whenever

$$\mathbf{T_{2,2}}(0, N) = 0. \tag{6.20}$$

Where $\mathbf{T_{2,2}}(0, N)$ is a submatrix of the full transfer matrix. Even though there are no spurious solutions present this method is unusable since the presence of both evanescent decaying and growing waves within the same transfer matrix leads to differences of 10^{20} between elements. The numerical work became unstable and finally the transfer matrix method was abandoned.

A method of separating the growing waves from the decaying waves can be obtained using scattering matrices instead of the transfer matrices. Scattering matrices can be obtained from our known transfer matrices as described in [14] by using:

$$\begin{pmatrix} \mathbf{a_n} \\ \mathbf{b_m} \end{pmatrix} = \mathbf{S}(m, n) \begin{pmatrix} \mathbf{a_m} \\ \mathbf{b_n} \end{pmatrix} \quad \text{and} \quad \begin{pmatrix} \mathbf{a_n} \\ \mathbf{b_n} \end{pmatrix} = \mathbf{T}(n, n+1) \begin{pmatrix} \mathbf{a_{n+1}} \\ \mathbf{b_{n+1}} \end{pmatrix} \tag{6.21}$$

These matrices are split into submatrices and we obtain,

$$\begin{pmatrix} \mathbf{T_{11}a_{n+1} + T_{12}b_{n+1}} \\ \mathbf{b_m} \end{pmatrix} = \mathbf{S(m, n)} \begin{pmatrix} \mathbf{a_m} \\ \mathbf{T_{21}a_{n+1} + T_{22}b_{n+1}} \end{pmatrix}. \tag{6.22}$$

We then have

$$\mathbf{S_{11}a_m} + \mathbf{S_{12}}(\mathbf{T_{21}a_{n+1}} + \mathbf{T_{22}b_{n+1}}) = \mathbf{T_{11}a_{n+1}} + \mathbf{T_{12}b_{n+1}} \Rightarrow \tag{6.23}$$

$$(\mathbf{S_{12}T_{21}} - \mathbf{T_{11}})\mathbf{a_{n+1}} = (\mathbf{T_{12}} - \mathbf{S_{12}T_{22}})\mathbf{b_{n+1}} - \mathbf{S_{11}a_m} \tag{6.24}$$

$$\mathbf{b_m} = \mathbf{S_{21}a_m} + \mathbf{S_{22}}(\mathbf{T_{21}a_{n+1}} + \mathbf{T_{22}b_{n+1}}) \Rightarrow \tag{6.25}$$

$$\mathbf{b_m} - \mathbf{S_{22}T_{21}a_{n+1}} = \mathbf{S_{21}a_m} + \mathbf{S_{22}T_{22}b_{n+1}} \tag{6.26}$$

So we obtain:

$$\begin{pmatrix} -\mathbf{S_{22}T_{21}} & 1 \\ \mathbf{S_{12}T_{21}} - \mathbf{T_{11}} & 0 \end{pmatrix} \begin{pmatrix} \mathbf{a_{n+1}} \\ \mathbf{b_m} \end{pmatrix} = \begin{pmatrix} \mathbf{S_{21}} & \mathbf{S_{22}T_{22}} \\ -\mathbf{S_{11}} & \mathbf{T_{12}} - \mathbf{S_{12}T_{22}} \end{pmatrix} \begin{pmatrix} \mathbf{a_m} \\ \mathbf{b_{n+1}} \end{pmatrix} \tag{6.27}$$

$$\begin{pmatrix} \mathbf{a_{n+1}} \\ \mathbf{b_m} \end{pmatrix} = \begin{pmatrix} 0 & (\mathbf{T_{11}} - \mathbf{S_{12}T_{21}})^{-1} \\ 1 & \mathbf{S_{22}T_{21}}(\mathbf{T_{11}} - \mathbf{S_{12}T_{21}})^{-1} \end{pmatrix} \begin{pmatrix} \mathbf{S_{21}} & \mathbf{S_{22}T_{22}} \\ \mathbf{S_{11}} & \mathbf{S_{12}T_{22}} - \mathbf{T_{12}} \end{pmatrix} \begin{pmatrix} \mathbf{a_m} \\ \mathbf{b_{n+1}} \end{pmatrix}. \tag{6.28}$$

From the above equation we can determine recursive formulas. Assume we know scattering matrix $\mathbf{S}(m,n)$ then,

$$\mathbf{S_{11}}(m,n+1) = (\mathbf{1} - \mathbf{T_{11}^{-1}S_{12}T_{21}})^{-1}\mathbf{T_{11}^{-1}S_{11}} \tag{6.29}$$

$$\mathbf{S_{12}}(m,n+1) = (\mathbf{1} - \mathbf{T_{11}^{-1}S_{12}T_{21}})^{-1}\mathbf{T_{11}^{-1}}(\mathbf{S_{12}T_{22}} - \mathbf{T_{12}}) \tag{6.30}$$

$$\mathbf{S_{21}}(m,n+1) = \mathbf{S_{21}} + \mathbf{S_{22}T_{21}S_{11}}(m,n+1) \tag{6.31}$$

$$\mathbf{S_{22}}(m,n+1) = \mathbf{S_{22}T_{22}} + \mathbf{S_{22}T_{21}S_{12}}(m,n+1) \tag{6.32}$$

Since $\mathbf{S}(m,m)$ must be identity matrices for arbitrary m we can construct scattering matrices for the whole structure. Using these formulas we construct the following matrices $\mathbf{S}(0,m)$ and $\mathbf{S}(m,N)$ and use these to determine the energy level by considering:

$$\mathbf{a_m} = \mathbf{S_{11}}(m,0)\mathbf{a_0} + \mathbf{S_{12}}(m,0)\mathbf{b_m} \tag{6.33}$$

$$\mathbf{b_m} = \mathbf{S_{21}}(m,N)\mathbf{a_m} + \mathbf{S_{22}}(m,N)\mathbf{b_N} \tag{6.34}$$

and by setting the incoming waves equal zero ($\mathbf{b_N} = \mathbf{a_0} = 0$) we get

$$\mathbf{0} = (\mathbf{1} - \mathbf{S_{12}}(0,m)\mathbf{S_{21}}(m,N))\mathbf{a_m}. \tag{6.35}$$

By iterating over energy we obtain bound states whenever this determinant is zero. Then we can find the coefficients as eigenvectors of for scattering matrices. The coefficients for the backwards traveling waves are given by

$$\mathbf{b_m} = \mathbf{S_{21}}(m,N)\mathbf{a_m}. \tag{6.36}$$

Using these we can completely determine the Ec, Lh and Sp bands.

The separated Hh can be solved by using a propagating trial function and the following boundary conditions obtained normally

$$\Psi_n = a_n e^{ik_n z} + b_n e^{-ik_n z} \quad \text{and} \quad \Psi_n = \Psi_{n+1} \quad \text{and} \quad h_{h,n}k_{n,\pm}\Psi_n = h_{h,n+1}k_{n+1,\pm}\Psi_{n+1} \tag{6.37}$$

Setting the incoming waves equal zero and solving the linear system of equation we obtain the transcendent equation

$$h_h^{In}k^{In}\frac{G-1}{G+1} = h_h^{Ga}k^{Ga}\frac{F-1}{F+1} \tag{6.38}$$

$$G = e^{2ik^{In}d_1}\frac{h_h^{In}k^{In} - h_h^{Al}k^{Al}}{h_h^{In}k^{In} + h_h^{Al}k^{Al}} \quad \text{and} \quad F = e^{-2ik^{Ga}d_2}\frac{h_h^{Ga}k^{Ga} - h_h^{Al}k^{Al}}{h_h^{Ga}k^{Ga} + h_h^{Al}k^{Al}} \tag{6.39}$$

With this equation we find the energy of the heavy-hole states.

6.3 Effectiv Hamiltonian for InAsGaSb

We are now ready to find the crossing between the first Hl state and the first electron like state. We fix the length of the GaSb layer $d_2 = 10$nm and vary the length of the InAs layer d_1. In this model the energy levels of the Hl state should be fixed, since these are localized in the GaSb layer. The Ec-Lh-Sp bands mix together and are present in both layers. A band is electron like if its mainly in the InAs layer and lighthole like if its mainly in the GaSb layer.

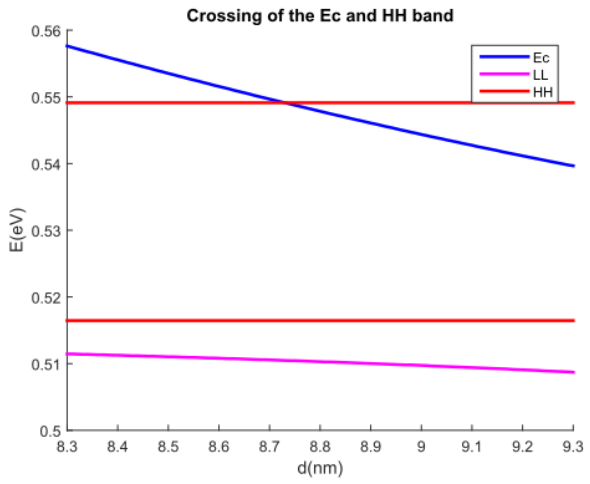

Figure 4: Energy levels of InAsGaSb quantum well. Crossing occurs at $d_c = 8.73$nm

Iterating over length of d_1 and solving the energy equations in numerically we obtain a crossing at $d_c \approx 8.73$nm. We determine it as the electron-like state by noticing that its energy drops rapidly when we increase d_1, while the lighthole like state which is more localized in GaSb, does not decrease so rapidly. These finding are in good agreement with the crossing found by [5] where they found it at $d_c \approx 9$nm. The placement of our Lh and Ec band is also in good agreement with the findings of [6]. We find the electron crossing with the second Hh state at $d = 14.5$nm where we leave the inverted state, since the Fermi energy then is placed between two Hh states. Getting a working script using these methods where first achieved at the end of this bachelor project. Sadly this did not leave time to find the coefficients of the wave functions which we would use to obtain the normalized states. With these we could easily identify the electron like state from the lighthole like state by looking at their distribution in the quantum well. We also need the wave functions to develop a effective model for the $k_{||}$ direction by doing a numerical integration across the well.

We will now discuss the form of the effective Hamiltonian without obtaining the precise coefficients. Following convention we will split our effective Hamiltonian into three parts so the total Hamiltonian is

$$H_{eff} = H_{BHZ} + H_{BIA} + H_{SIA}, \tag{6.40}$$

where the first term is the same Hamiltonian as obtained in the HgTe model. There would be similar contributions as calculated in HgTe but here we also include the Split-Off hole.

The H_{SIA} is the Structural Inversion Asymmetry (SIA) terms. We have a off-diagonal contribution from the Ec/Lh, Ec/Sp and Lh/Sp couplings. H_{BIA} is the Bulk Inversion Asymmetric contribution and is simply the states interacting through the B dependent terms. These contributions takes the form

$$H_{Sia} = \begin{pmatrix} 0 & 0 & \xi_e k_- & 0 \\ 0 & 0 & 0 & 0 \\ \xi_e k_+ & 0 & 0 & 0 \\ 0 & 0 & 0 & 0 \end{pmatrix}, \quad H_{Bia} = \begin{pmatrix} 0 & 0 & \Delta_0 k_- & 0 \\ 0 & 0 & 0 & 0 \\ \Delta_0 k_+ & 0 & 0 & 0 \\ 0 & 0 & 0 & 0 \end{pmatrix} \tag{6.41}$$

$$\xi_e = \int_{-\infty}^{\infty} dz \left[\langle Ec| \frac{1}{\sqrt{3}} T |LL\rangle + \langle Ec| \sqrt{\frac{2}{3}} T |SP\rangle + \langle LL| \sqrt{\frac{2}{3}} R |SP\rangle \right], \tag{6.42}$$

$$\Delta_e = \int_{-\infty}^{\infty} dz \left[\langle Ec| \frac{1}{\sqrt{3}} V |LL\rangle + \langle Ec| \sqrt{\frac{2}{3}} V |SP\rangle \right]. \tag{6.43}$$

Since we want to describe our effective Hamiltonian in terms of k_x, k_y to second order we neglect off-diagonal contributions in second order of k_x, k_y, since they will enter the energy as a fourth order contribution. In this model we need to be really careful about the parity of the states. The Hh is still antisymmetric, but classifying the hybridized Ec-Lh-Sp hole is more tricky and would require detailed calculations from its components in each material.

In [5] they found a Hamiltonian which contains additional terms where some can be contributed to the Rashba effect which we will discuss shortly in the next chapter. They also find a k independent contribution to the off-diagonal elements. This contribution cannot be achieved by second order perturbation. In [5] they ascribe it to BIA, but such terms should always be k_x or k_y dependent if they arise from $k \cdot p$ theory. Other authors ascribe it to SIA breaking [7] so there seems to be some confusion on the subject.

7 2d topological insulators

In following subsection we will derive some of the most important characteristics of the topological insulator. First we derive the helical edge states and show that their is only one solution for spin-up and -down states for a interface. Then by studying the Time-reversal (TR) we conclude that these form a topological protected Kramer's pair. Then by finding representations for TR and parity (P) we discuss possible terms that could be added to the BHZ model and what symmetries these break/conserve. Finally we discuss macroscopic transport measurements

and how one can measure the helical edge states. We also find the existence of a quantized transverse spin current, known as the quantum spin hall effect.

The tightbinding model is a easy way of solving topological systems and using this method we have obtained plots of most effects described in the next sub-sections. An explanation of the tight-binding theory is provided in appendix.B.

7.1 Egde states

In topological insulators one obtains edge states while conserving the TR symmetry which leads to TR protected edge channels [7]. To study these effects we will use the BHZ model Eq.5.23 which will expressed in terms of Pauli matrices as

$$H_{BHZ} = \begin{pmatrix} H(\mathbf{k}) & 0 \\ 0 & H^*(-\mathbf{k}) \end{pmatrix}, \quad H(\mathbf{k}) = \sum_i d_i \sigma_i \tag{7.1}$$

$$d_0 = C + Dk_{||}^2, \quad d_x = Ak_x, \quad d_y = Ak_y, \quad d_z = M + Bk_{||}^2. \tag{7.2}$$

Following the steps of [15] we seek edge state solutions at a open interfaces. We adopt periodic boundary conditions for x so k_x will still be a good quantum number and we place the open interface at $y = 0$ and substitute $y \to -i\partial_y$. We solve the spin up part of the Hamiltonian since the spin down part follows trivially. Since we are looking for edge states we use the trial function

$$\Psi_\uparrow = \sum_n \mathbf{f_n} e^{\gamma_n y}, \tag{7.3}$$

and using the now familiar equations for γ and eigenvectors we obtain

$$\gamma^2 = k_x^2 + F \pm \sqrt{F^2 - \frac{M^2 - E^2}{B_+ B_-}} \quad \text{and} \quad \mathbf{f_n} = \begin{pmatrix} -A(\gamma_n + k_x) \\ M - B_+(\gamma_n^2 - k_x^2) - E \end{pmatrix} \tag{7.4}$$

$$F = \frac{2(MB + ED) - A^2}{2B_+ B_-}, \quad B_+ = B + D, \quad B_- = B - D. \tag{7.5}$$

For a open interface we know that $\mathbf{\Psi}(0) = \mathbf{\Psi}(\infty) = 0$, so there are only two backwards decaying waves. At $y = 0$ we find

$$0 = \mathbf{f_1} + \mathbf{f_2} \quad \to \quad \frac{M - B_+(\gamma_1^2 - k_x^2) - E}{-A(\gamma_1 + k_x)} = \frac{M - B_+(\gamma_2^2 - k_x^2) - E}{-A(\gamma_2 + k_x)}, \tag{7.6}$$

which we solve for E:

$$E = M - B_+ k_x^2 - B_+ \gamma_1 \gamma_2 - B_+(\gamma_1 + \gamma_2) k_x. \tag{7.7}$$

We now set $k_x = 0$ to find the necessary conditions for the existences of edge states in the center of the gap. Using Eq.7.4 we get

$$E = M - B_+ \gamma_1 \gamma_2 = M - B_+ \sqrt{\frac{M^2 - E^2}{B_+ B_-}} \Rightarrow M - E = B_+^2 - \frac{M - E}{B_+ B_-} \Rightarrow E = -\frac{D}{B} M \tag{7.8}$$

$$\gamma_1 \gamma_2 = \frac{M - E}{B_+} = \frac{M}{B} \frac{D_+}{D_+} = \frac{M}{B} \tag{7.9}$$

$$(\gamma_1 + \gamma_2)^2 = \gamma_1^2 + \gamma_2^2 + 2\gamma_1 \gamma_2 = 2F + 2\frac{M - E}{B_+} = \frac{A^2}{B_+ B_-} \Rightarrow \gamma_1 + \gamma_2 = \sqrt{\frac{A^2}{B_+ B_-}} \tag{7.10}$$

To have a edge state at $k_x = 0$ we need γ_1 and γ_2 to be real positive numbers. So we obtain the following conditions for existence of edge states

$$\frac{M}{B} > 0 \quad \text{and} \quad \frac{A^2}{B_+ B_-} > 0 \tag{7.11}$$

We see from tabel.2 that the inverted band gap of HgTe supports an edge state while the normal gap does not. Now we expand our dispersion relation to first order in k_x:

$$E = E_0 + E_1 k_x + O(k_x^2), \quad E_1 = \frac{dE}{dk_x}\bigg|_{k_x=0} = -B_+ \frac{d(\gamma_1\gamma_2)}{dk_x}\bigg|_{k_x=0} - B_+(\gamma_1+\gamma_2)|_{k_x=0} = \tag{7.12}$$

$$-B_+\left[\frac{1}{2\gamma_1\gamma_2|_{k_x=0}}\frac{d}{dk_x}\frac{M^2-E^2}{B_+B_-} + B_+A\frac{1}{\sqrt{B_+B_-}}\right] = -B_+\left[\frac{-BE|_{k_x=0}}{MB_+B_-}\frac{dE}{dk_x}\bigg|_{k_x=0} + A\sqrt{\frac{B_+}{B_-}}\right] = \tag{7.13}$$

$$-B_+\left[\frac{D}{B_+B_-}\frac{dE}{dk_x}\bigg|_{k_x=0} + A\sqrt{\frac{B_+}{B_-}}\right] \Rightarrow \frac{dE}{dk_x}\bigg|_{k_x=0} = A\sqrt{\frac{B_+}{B_-}}\left(1+\frac{D}{B_-}\right)^{-1} = A\frac{\sqrt{B_+B_-}}{B} = \mathrm{sgn}(B)A\sqrt{1-\frac{D^2}{B^2}} \tag{7.14}$$

Since our model is already based on expansion around a small k_x we will only go to first order in k_x. So the dispersion relation and effective velocity of edge states is given by

$$E_{\uparrow,\downarrow=\pm} = -\frac{DM}{B} \pm \mathrm{sgn}(B)A\sqrt{1-\frac{D^2}{B^2}}k_x \quad \text{and} \quad v_{\uparrow,\downarrow=\pm} = \pm\mathrm{sgn}(B)A\sqrt{1-\frac{D^2}{B^2}}. \tag{7.15}$$

The two spin blocks of the BHZ model have different sign for the A term, so the solutions for different spin runs in opposite directions along the interface. Such states are known as a helical pair. These edge states are very different from the edge states of the quantum hall phase where all edge states run in the same direction. This is due to the unique features of the topological insulator which creates edge states without breaking TR symmetry. The two helical edge states of a topological insulator are shown in fig.5.

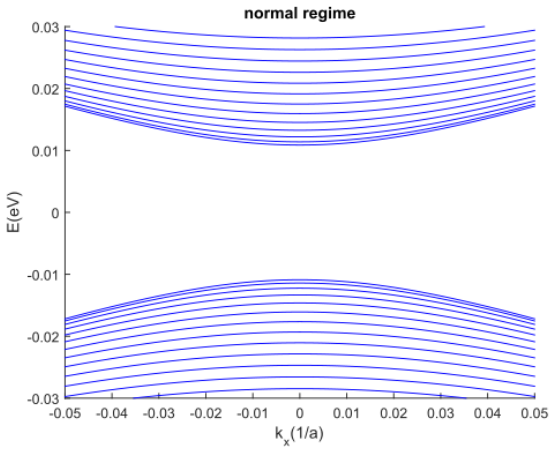

(a) HgTe at L=6nm with 400 unit cells along the x-axis.

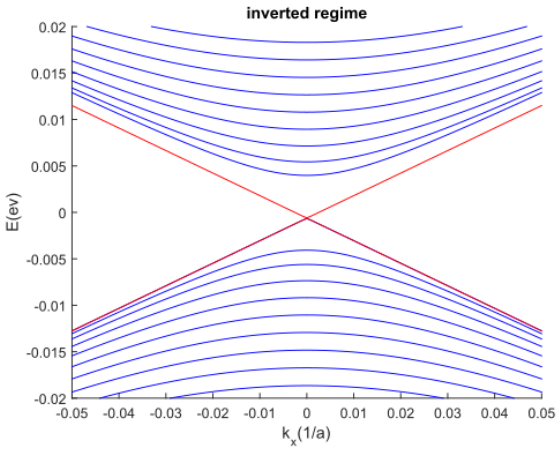

(b) HgTe at L=7nm with 400 unit cells along the x-axis. The helical egde states are shown in red.

Figure 5: The topological state.

7.2 Time Reversal symmetry

Many of the unique features of helical edge states depends on TR symmetry. We will, based on the work of [8], present some of the most striking features of unbroken TR symmetry.

We define TR symmetry as: $T : t \to -t$ and applying it yields

$$TxT^{-1} = x, \quad TpT^{-1} = -p, \quad T\mathbf{S}T^{-1} = -\mathbf{S}. \tag{7.16}$$

Where $\mathbf{S}$ is the spin operator for a particle, so S returns the spin quantum number when used on a state. The last relation is true, since spin is a internal angular moment. Then by using TR on the fundamental commutator we obtain

$$T\left[x,p\right]T^{-1} = Ti\hbar T^{-1} = -\left[x,p\right] = -i\hbar \quad \to \quad TiT^{-1} = -i \tag{7.17}$$

So a given representation of time reversal symmetry must contain the complex conjugation operator. Since it must also reverse the direction of spin it can be represented by a π rotation around a spin-axis and following convention we choose the y-axis

$$T = e^{-i\pi S_y}K \Rightarrow T\cdot T = e^{-i2\pi S_y} \Rightarrow T_{int}^2 = 1, \quad T_{\frac{1}{2}int}^2 = -1 \tag{7.18}$$

Where K is the complex conjugation operator and int stands for integer spin space and $\frac{1}{2}int$ is for half integer spin space. In general T can be represented by $T = UK$ where U is a unitary matrix. For a half-integer spin space we get

$$T^2 = UU^* = U(U^T)^{-1} = -1 \Rightarrow U = -U^T \tag{7.19}$$

This important result leads to Kramer's degeneracy for TR symmetric half-integer spin spaces. Consider a TR invariant Hamiltonian H with a eigenstate $|\psi\rangle$, then $|\phi\rangle = T|\psi\rangle$ must also be an eigenstate. We check if these states are orthogonal:

$$\langle\psi|T\psi\rangle = \sum_{n,m} \psi_m^* U_{nm} \psi_n^* = -\sum_{n,m} \psi_n^* U_{mn} \psi_m^* = -\langle\psi|T\psi\rangle = 0 \tag{7.20}$$

This implies that if our Hamiltonian is TR symmetric then each state is doubly degenerate with their partner given by TR symmetry. We let T operate on a TR invariant Hamiltonian:

$$TH(k)T^{-1} = H^*(-k) = H(k) \tag{7.21}$$

So if TR symmetry is present we must have spin degeneracy at $k = 0$. Spin-up and -down must then be reflections of each other through the $k = 0$ line.

Looking back at our BHZ Hamiltonian (Eq.7.1) we identify the spin-down block to be the TR transformed of the spin-up block. It then follows that the helical pair found in the previous section form a Kramer's pair.

Now lets consider scattering between Kramer pairs resulting from TR invariant interactions $V = TVT^{-1}$:

$$\langle T\psi|\, V\, |\psi\rangle = \sum_{n,m,j} U_{mj}^* \psi_j V_{mn} \psi_n = \sum_{n,m,j} U_{jm}^\dagger \psi_j V_{mn} \psi_n = \sum_{n,m,j} U_{jm}^\dagger \psi_j T V_{m,n} T^{-1} \psi_n \tag{7.22}$$

$$= \sum_{n,m,j,r,q} \psi_j U_{jm}^\dagger U_{mr} K V_{rq} K U_{qn}^\dagger \psi_n = -\sum_{n,j,r,q} \psi_j \delta_{jr} V_{rq}^* U_{nq}^* \psi_n = -\sum_{n,m,j} \psi_j V_{jq}^* U_{nq}^* \psi_n \tag{7.23}$$

$$= -\sum_{q,j,n} U_{nq}^* \psi_q V_{qj} \psi_j = -\langle T\psi|\, V\, |\psi\rangle = 0 \tag{7.24}$$

This property is known as the TR protection, since it implies that helical states cannot scatter into their Kramer's partner if the interaction is TR symmetric. It also states that no gap can be created between a Kramer's pair without a perturbation breaking TR symmetry. If we were to calculate the probability that n states to scatter into n time reversal partners we would obtain a factor -1^n. So the states are only protected from odd particle scattering events.

If our Hamiltonian is invariant to both TR and parity (P) we obtain: $PTH(k)T^{-1}P^{-1} = PH(-k)^*P^{-1} = H(k)^* = H(k)$. Which implies that the Kramer's pair is degenerate at all k.

7.3 Representations of the BHZ model.

In order to investigate the symmetries of the BHZ model we will construct matrix representations for TR and P [8]. Using these we can determine what perturbations that breaks these symmetries. We are then able to guess effects of different kinds of perturbations without doing full band calculations.

We utilize a notation that only considers the symmetries of given terms. Here $d(k)$ just represent the order of k. In this notation the BHZ Hamiltonian and its TR transformed is expressed as

$$H_{BHZ}(k) = d(k^2)\sigma_0 \otimes (\tau_0 + \tau_z) + d(k)\sigma_z \otimes \tau_x + d(k)\sigma_0 \otimes \tau_y, \tag{7.25}$$

$$H_{BHZ}^*(-k) = d(k^2)\sigma_0 \otimes (\tau_0 + \tau_z) - d(k)\sigma_z \otimes \tau_x + d(k)\sigma_0 \otimes \tau_y, \tag{7.26}$$

with τ_i as a Pauli matrix describing the electron/hole subspace, while σ describe spin-up/spin-down subspace. For a matrix to a representation of TR it needs to transform the Hamiltonian the same way as TR. This transformation should preserve all terms except $\tau_z \otimes \sigma_x$ which changes sign. Since τ and σ belong to different subspaces we have

$$(\sigma_i \otimes \tau_\mu)(\sigma_j \otimes \tau_\nu) = \sigma_i\sigma_j \otimes \tau_\mu\tau_\nu, \tag{7.27}$$

and since Pauli matrices transform as

$$\sigma_j\sigma_i\sigma_j = -\sigma_i \quad \text{and} \quad \sigma_j\sigma_j\sigma_j = \sigma_j, \tag{7.28}$$

we can determine how the combined space transforms. As an example we let the matrix $A = \sigma_y \otimes \tau_z$ be transformed by $B = \sigma_y \otimes \tau_x$:

$$BAB^{-1} = (\sigma_y\sigma_y\sigma_y^{-1}) \otimes (\tau_x\tau_y\tau_x^{-1}) = -\sigma_y \otimes \tau_y. \tag{7.29}$$

Using these relations we find representations for the TR symmetry which transform Eq.7.25 into Eq.7.26. These are

$$T_1 = -i\sigma_y \otimes \tau_0 K \quad \text{and} \quad T_2 = \sigma_x \otimes \tau_0 K. \tag{7.30}$$

Since this implies that $T_1^2 = -1$ and $T_2^2 = 1$ and we know that our electrons are half-integer the correct one for our system must be T_1. Because of the parity of our atomic s and p basis the parity representation must take the form $P = \sigma_z$ in basis. Expanding this for the full BHZ model with spin:

$$P = \sigma_0 \otimes \tau_z. \tag{7.31}$$

Applying this on our Hamilton $THT^{-1} = 1$, the BHZ model describes a inversion invariant system. So the edge states are degenerate for all k. We can now verify it a given perturbation breaks either TR or parity symmetry by considering the transformations: PHP^{-1} and THT^{-1}.

In the InAsGaSb quantum well we obtained off-diagonal terms Eq.6.41 which we could attribute to the breaking of parity. Lets consider how they transform. We define $\Delta = \phi_e + \Delta_0$ and express H_{BIA} and H_{SIA} as

$$H_{off} = H_{SIA} + H_{BIA} = \frac{\Delta}{2} k_x \sigma_x \otimes (\tau_0 + \tau_z) + \frac{\Delta}{2} k_y \sigma_y \otimes (\tau_0 + \tau_z). \tag{7.32}$$

Since P and T sends $k \to -k$ they transform as $TH_{off}T^{-1} = 1$ and $PH_{off}P^{-1} = -1$. So these terms does not break TR symmetry but do break inversion symmetry. We name this type one inversion asymmetry. Following the previous discussion these terms will lift the spin degeneracy away from the $k = 0$ point, but since the gap is TR protected it will remain unaffected so our InAsGaSb model can contain topological states. The effects of this perturbation is shown at fig.6.

We are able to construct additional terms that keep TR symmetry but breaks inversion symmetry. One of the most interesting is

$$H_P = \Delta_1 \sigma_y \otimes \tau_y \tag{7.33}$$

which clearly breaks parity but because of the double complex conjugation it keeps TR symmetry. Since this term is k independent it will produce a gap, even at $k = 0$. But this cannot destroy the topological order. It can be seen at fig.6 that this perturbation separates the TR invariant point for the two boundaries which forces the crossings of the boundary terms to happen at $k \neq 0$. We call this type two inversion asymmetry.

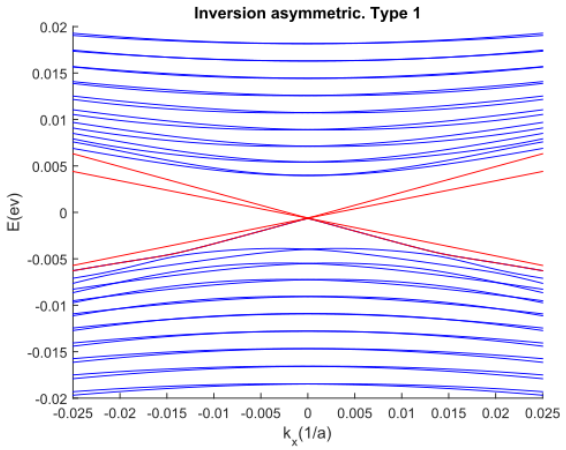

(a) HgTe at L=7nm with 400 unit cells along the x-axis. The helical edge states are shown in red. Here we have $\Delta_0 = 0.1$eVnm

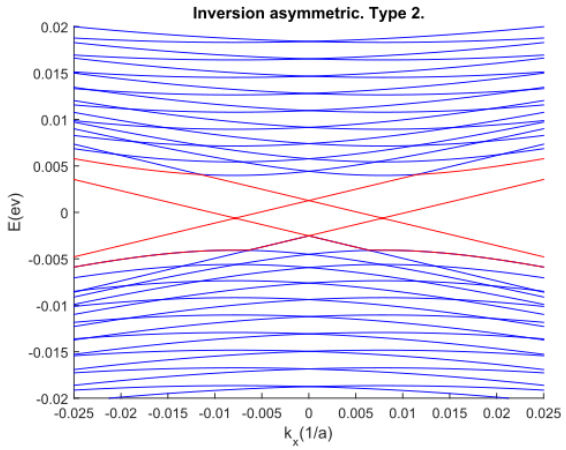

(b) HgTe at L=7nm with 400 unit cells along the x-axis. The helical egde states are shown in red. Here we have $\Delta_1 = 0.003$eV

Figure 6: Broken inversion symmetry.

By applying fields across our quantum well we can also break symmetries. Application of a B-field should break time-reversal symmetry, while a E-field should break inversion symmetry. We now consider these two effects expressed as

$$H_Z = g^* \sigma \cdot B \quad \text{and} \quad H_R = \alpha(\sigma \cdot E \times k. \tag{7.34}$$

Where g^* is the effective g factor and α the effective Rashba coefficient for a given band. The second term is the Rashba term arising from the spin-orbit coupling (Eq.3.23) when considering perturbation by a E-field to first order ($V = V_0 + E \cdot r$) [20]. The Rashba contribution is especially important for the InAsGaSb well, since the broken gap produces a intrinsic electrical field which couples to spin. The effective factors for such contributions

can be found using Lowdin perturbation on our Hamilton Eq.3.41 to small order, but this is beyond the scope of this project [20].

Since these terms only couple spin between states we can determine their position in the BHZ Hamiltonian. Using the symmetry notation and allowing the fields to point in all directions we get

$$H_Z = d(0)(\sigma_x + \sigma_y + \sigma_z) \otimes (\tau_0 + \tau_z) \quad \text{and} \quad H_R = d(k)(\sigma_x + \sigma_y + \sigma_z) \otimes (\tau_0 + \tau_z), \tag{7.35}$$

which transforms as $PH_ZP^{-1} = H_Z$, $TH_ZT^{-1} = -H_Z$, $PH_RP^{-1} = -H_R$ and $TH_RT^{-1} = H_R$. Just as expected the Zeeman effect breaks TR but keeps inversion. While the Rashba term breaks inversion while keeping TR. This could also been seen from their different k dependence.

So by applying a E field we can change the structure of the topological states without destroying the topological gap and by applying a B field we can open a gap between the Kramer's pair.

7.4 Finite Size effect

Finally we will talk about the finite size effect. We showed earlier that there are precisely one Kramer's pair at each boundary. For normal bulk states there are always an even number of Kramer pairs and this induces a gap since they interact. In real systems our boundary at each end of the system are not infinitely separated from each other. So our previous calculations for a isolated open boundary is not completely valid. In real systems a gap is formed from the interaction of Kramer pairs at each end of the system, which is proportional to the overlap of the wave-functions. This will produces a gap intersection without breaking time reversal symmetry. In this section we want to find the characteristic length scale of a helical state so we can estimate the effect of finite size gap openings.

From the definition of edge states we know that they decay as $e^{\gamma_S y}$ where we have chosen $\gamma_L > \gamma_S$. By using Eq.7.15 we find our γ's up to second order in k_x,

$$\gamma_1\gamma_2 = \gamma_1\gamma_2|_{k_x=0} + \left.\frac{d(\gamma_1\gamma_2)}{dk_x}\right|_{k_x=0} k_x + \left.\frac{d^2(\gamma_1\gamma_2)}{d^2k_x}\right|_{k_x=0} k_x^2 = \frac{M}{B} + \frac{D}{B_+B_-}\left.\frac{dE}{dk_x}\right|_{k_x=0} k_x - k_x^2 = \frac{M}{B} + \frac{2DN}{B}k_x - k_x^2 \tag{7.36}$$

$$\gamma_1 + \gamma_2 = \gamma_1 + \gamma_2|_{k_x=0} + \left.\frac{d(\gamma_1+\gamma_2)}{dk_x}\right|_{k_x=0} k_x + \left.\frac{d^2(\gamma_1+\gamma_2)}{d^2k_x}\right|_{k_x=0} k_x^2 = 2N \tag{7.37}$$

Where $N = A/2\sqrt{B_+B_-}$. Now we solve for γ,

$$\gamma_1(2N - \gamma_1) = \frac{M}{B} + \frac{2DN}{B}k_x - k_x^2 \Rightarrow \gamma_1 = N \pm \sqrt{N^2 - \frac{M}{B} - \frac{2DN}{B}k_x + k_x^2} = N \pm \sqrt{N^2 + (k_x - k_+)(k_x - k_-)} \tag{7.38}$$

$$\text{with} \quad k_\pm = \frac{DN}{B} \pm \sqrt{\frac{D^2N^2}{B^2} + \frac{M}{B}} \tag{7.39}$$

We define the anti-localization length as $l = \gamma_S^{-1}$ where γ_S is the smallest of γ. then

$$l^{-1} = N - \sqrt{N^2 + (k_x - k_+)(k_x - k_-)} \tag{7.40}$$

When the anti-localization length goes to ∞ our edge states evolve into bulk states [15], which happens at $k_x = k_\pm$. These are points where the edge state meets the top or bottom bulk bands. The size of the finite size gap decrease as L_y is increased. At the $k_x = 0$ point the characteristic length is

$$l = \left[N - \sqrt{N^2 - \frac{M}{B}}\right]^{-1}. \tag{7.41}$$

From our HgTe parameters we find $l = 116.45nm$ for $L = 7mn$. Since most terminal structures used for transport measurements are hundreds of micrometers wide [1] this effect is negligible for HgTe. The effects of finite size on the topological system can be seen at fig.7.

7.5 Transport

The topological state has a odd number of Kramer's pairs at each interface so it behaves as a 1.d helical liquid. [7]. But all these effects are microscopic and we need a macroscopic way of determining if our system is indeed in the topological phase. This can be done by transport measurements.

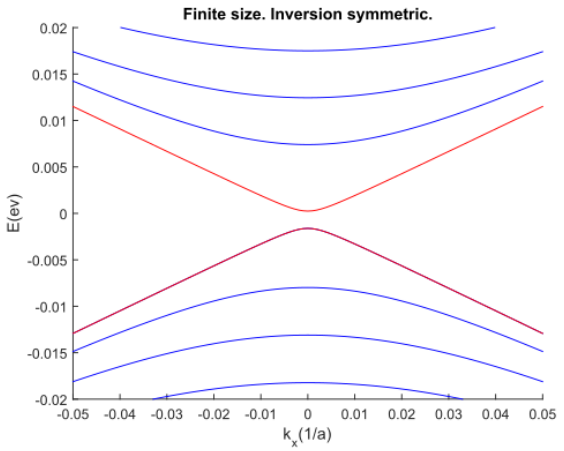

(a) HgTe at L=6nm with 150 unit cells along the x-axis. The helical egde states are shown in red.

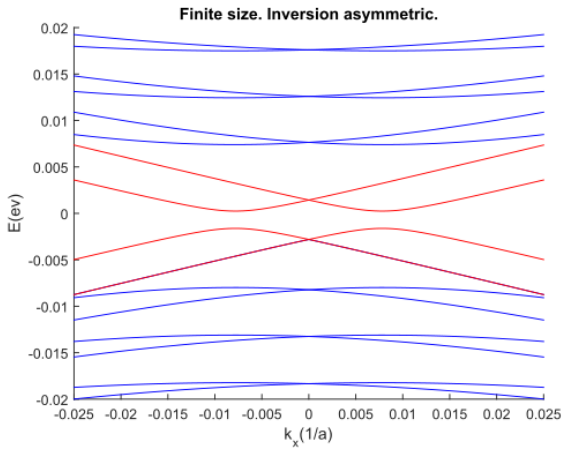

(b) HgTe at L=7nm with 150 unit cells along the x-axis. The helical egde states are shown in red. $\Delta_1 = 0.003eV$

Figure 7: Finite size effect.

In transport measurements one sends a current through the system and measures the conductivity. Consider a topological insulator where x is large enough to ignore finite size effect, so that we obtain a pair of gap-less edge states. We set the temperature close to zero and the Fermi energy is placed in the gap of the bulk states so they cant contribute to transport. All contributions now stems from edge states. Consider a two terminal device with a potential difference between. Using Landau formalism we express the current as

$$I = -ev_{eff}T\delta N, \tag{7.42}$$

where v_{eff} is the velocity of charge carriers, δN is the density of charge carriers and T is the probability that a electron will transmit from one end to the other. Since these states are time-reversal protected from most scattering and we assume the device to be small we set $T \approx 1$. We assume the potential difference to be small so,

$$\delta N \approx \frac{dN}{dE}\delta E = -e\frac{dN}{dk}(V_l - V_r) = -e\frac{dN}{dE}\frac{dk}{dE}(V_l - V_r) = -\frac{e}{2\pi}\frac{dk}{dE}(V_l - V_r), \tag{7.43}$$

where V_l and V_r is the voltage at the left and right terminal. Using the definition of $v_{eff} = dE/\hbar dk$, we obtain the conductance G from the two channels as

$$I_{\uparrow,\downarrow} = \frac{e^2}{h}(V_l - V_r) \quad \rightarrow \quad I_c = I_{c,\uparrow} + I_{c,\downarrow} = 2\frac{e^2}{h}(V_l - V_r) \quad \rightarrow \quad G = 2\frac{e^2}{h}. \tag{7.44}$$

with conductance quantized to e^2/h. If this quantization is found then current is transfered by 1.d edge states. Unfortunately the normal quantum hall edge states, arising from landau level crossing the Fermi level, gives the same result, if the number of crossing is $\nu = 2$. So we want to obtain a measurement that separates the quantum spin hall state from the quantum hall state. This can be achieved in four terminal measurements. In order to show this we will use Landau-Buttiker formalism [7] which explicitly accounts for all contributions in a given terminal. In this notation the current at a terminal is given by

$$I_i = \frac{e^2}{h}\sum_j T_{i,j}(V_i - V_j). \tag{7.45}$$

Different spin gives different contributions since they run in opposite directions so we obtain:

$$\begin{pmatrix} I_1^{\uparrow} \\ I_2^{\uparrow} \\ I_3^{\uparrow} \\ I_4^{\uparrow} \end{pmatrix} = \frac{e^2}{h}\begin{pmatrix} -1 & 0 & 0 & 1 \\ 1 & -1 & 0 & 0 \\ 0 & 1 & -1 & 0 \\ 0 & 0 & 1 & -1 \end{pmatrix}\begin{pmatrix} V_1 \\ V_2 \\ V_3 \\ V_4 \end{pmatrix} \quad \text{and} \quad \begin{pmatrix} I_1^{\downarrow} \\ I_2^{\downarrow} \\ I_3^{\downarrow} \\ I_4^{\downarrow} \end{pmatrix} = \frac{e^2}{h}\begin{pmatrix} -1 & 1 & 0 & 0 \\ 0 & -1 & 1 & 0 \\ 0 & 0 & -1 & 1 \\ 1 & 0 & 0 & -1 \end{pmatrix}\begin{pmatrix} V_1 \\ V_2 \\ V_3 \\ V_4 \end{pmatrix}. \tag{7.46}$$

The total transport is then given by the sum of these matrices. Since the quantum hall states run in the same direction and our the topological run in opposite we find,

$$\begin{pmatrix} I_1 \\ I_2 \\ I_3 \\ I_4 \end{pmatrix}_{SH} = \frac{e^2}{h}\begin{pmatrix} -2 & 1 & 0 & 1 \\ 1 & -2 & 1 & 0 \\ 0 & 1 & -2 & 1 \\ 1 & 0 & 1 & -2 \end{pmatrix}\begin{pmatrix} V_1 \\ V_2 \\ V_3 \\ V_4 \end{pmatrix} \quad \text{and} \quad \begin{pmatrix} I_1 \\ I_2 \\ I_3 \\ I_4 \end{pmatrix}_{H} = 2\frac{e^2}{h}\begin{pmatrix} -1 & 1 & 0 & 0 \\ 0 & -1 & 1 & 0 \\ 0 & 0 & -1 & 1 \\ 1 & 0 & 0 & -1 \end{pmatrix}\begin{pmatrix} V_1 \\ V_2 \\ V_3 \\ V_4 \end{pmatrix}. \tag{7.47}$$

Where SH is for spin hall, while H is for hall. We now send current from I_1 to I_3.

$$I_{2,H} = 2\frac{e^2}{h}(V_3 - V_2) = 0 \quad \text{and} \quad I_{2,SH} = \frac{e^2}{h}(V_1 + V_3 - 2V_2) = 0. \tag{7.48}$$

From which we obtain the conductance,

$$I_{1,H} = 2\frac{e^2}{h}(V_3 - V_1) \to G_H = 2\frac{e^2}{h} \quad \text{and} \quad I_{1,SH} = \frac{e^2}{h}(V_2 + V_4 - 2V_1) = \frac{e^2}{h}(V_3 - V_1) \to G_{SH} = \frac{e^2}{h}. \tag{7.49}$$

So by finding the conductance under these conditions one can separate the quantum hall state from the topological state.

Finally we discuss the quantum spin hall effect. Consider the 4-terminal setup for SH with $V_2 = V_4 = 0$ and $V_1 = -V_3 \neq 0$. To obtain the spin conductance we change units by multiplying with $\hbar/2e$ and since helical states of different spin travel in opposite direction we get the total spin current to be

$$I_S = I_S^{\uparrow} - I_S^{\downarrow} = \begin{pmatrix} I_1 \\ I_2 \\ I_3 \\ I_4 \end{pmatrix}_S = \frac{e}{4\pi} \begin{pmatrix} 0 & 1 & 0 & -1 \\ -1 & 0 & 1 & 0 \\ 0 & -1 & 0 & 1 \\ 1 & 0 & -1 & 0 \end{pmatrix} \begin{pmatrix} V_1 \\ V_2 \\ V_3 \\ V_4 \end{pmatrix} \Rightarrow I_{2,S} = \frac{e}{4\pi}(V_3 - V_1) \Rightarrow G_2^{\uparrow} = \frac{e}{4\pi} \tag{7.50}$$

So like the hall state where there is a transverse current, there is a quantized transverse spin current in the quantum spin hall state. This new effect has potential applications in the construction of spin based systems. From these calculations we can conclude that the HgTe well can be used to obtain isolated spin currents.

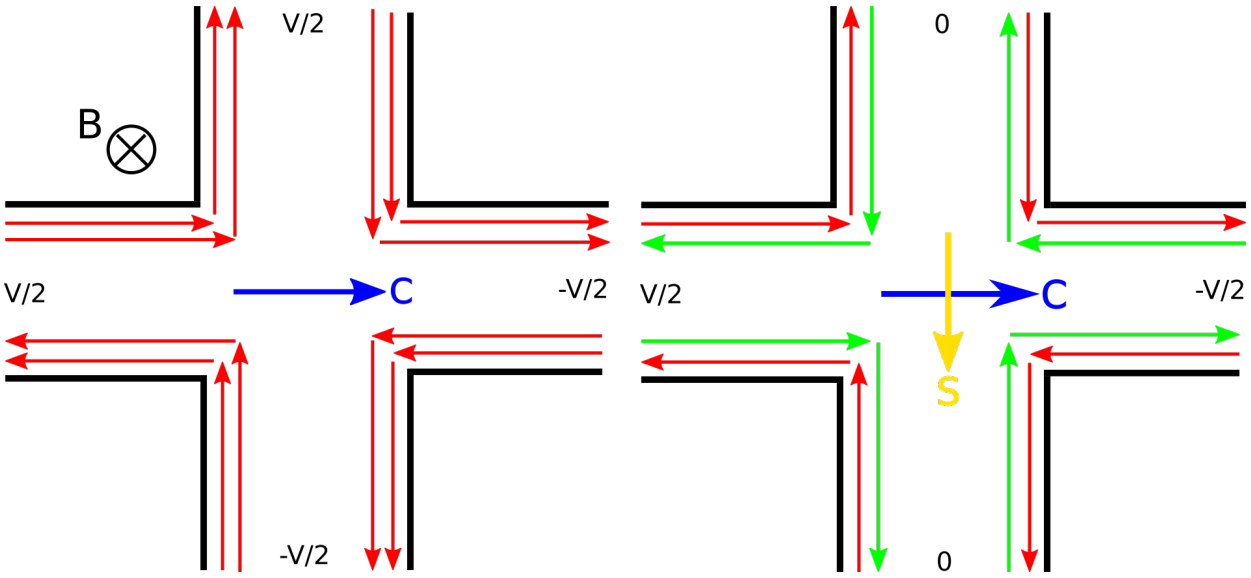

(a) The quantum hall effect with $\nu = 2$. C is the charge current and B is the magnetic field.

(b) The quantum spin hall effect. Different spins is colored different colors. C is for charge current. S is for spin current

Figure 8: The 4 terminal setup.

8 Conclusion

In this thesis we have used $k \cdot p$ theory and selection rules to derive a Hamiltonian for the zinc blende crystal up to second order in k. We use this Hamiltonian to obtain envelope functions in each material and by developing proper boundary conditions we are able to obtain the band structure of two quantum wells. We then obtain a inverted regime for each of these wells: HgTe is inverted for 6.76nm$< L <$ 8.66nm and InAsGaSb is inverted for 8.73nm$> d >$ 14.5nm. We then show that this inverted regime leads to the formation of exactly one pair of helical edge states at a open interface. This helical pair is shown to be protected from scattering and gap-opening by Time reversal symmetry. For numerical work on InAsGaSb wells the transfer matrix formalism proved to be unstable, this made it necessary to derive scattering matrices to obtain numerical stability. If we had more time we would calculate the envelope functions for InAsGaSb numerically, in order to derive an effective Hamiltonian describing the band interaction near the crossing. From this Hamiltonian we would be able to obtain helical edge states with broken inversion symmetry.

By developing an effective model for the HgTe quantum well we obtained a characteristic length of 116.45nm for the helical edge states. Since most terminal structures are of the order of hundreds of micrometers, we conclude that the helical edge states of HgTe are measurable by transport experiments and that we can achieve the quantum spin hall effect in HgTe systems.

Further research into the inversion asymmetric contributions, especially from the Rashba effect, is also needed in order to understand the InAsGaSb topological insulating state.

Appendices

A Crystal group theory of the Zinzblende structure

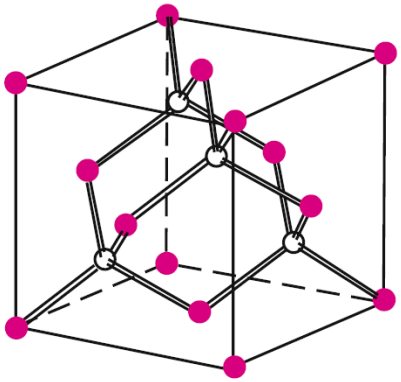

(a) Zinc blende conventionell cell. This is taken [10]. [9]

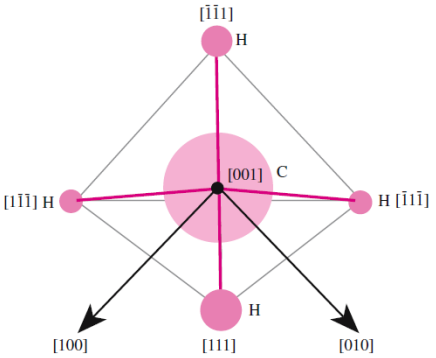

(b) The zinc blende tetrahedron defined by three orthogonal planes. This is taken from [10]. (1,0,0),(0,1,0),(0,0,1)

From theory described in [10] and [10] we provide a quick review of crystal group theory. The zinc blende structure consist of a tetrahedron with a atom in the center and four atoms of a different type located in each corner of the tetrahedron. The primitive lattice vectors of the system are not orthogonal and point to the nearest atoms, which are not the ones we will use to describe the tetrahedron. Instead we will use the orthogonal basis of the square unit cell. The four corner sites of the tetrahedron are described by the vectors [1,1,1],[1,-1,-1],[-1,1,-1],[-1,-1,1]. The zinc blende crystal has 3 translational symmetries along the 3 cube axis. It is also symmorphic which means that the order of rotation and translation are irrelevant. Therefore these can be split into two independent subgroups, here we will only deal with rotations and reflections, as the Bloch formalism covers the translational symmetries. The point group symmetries of the tetrahedron are:

- E: Identity transformation. 1 total.
- C_2: π rotation around a unit axis: [1,0,0], [0,1,0] or [0,0,1]. 3 total.
- C_3: $\frac{2\pi}{3}$ and $-\frac{2\pi}{3}$ rotations around each atom:[1.1.1],[1,-1,-1],[-1,1,-1] or [-1,-1,1]. 8 total.
- σ: reflection around the planes. [1,1,0],[1,-1,0],[1,0,1],[1,0,-1],[0,1,1] or [0,1,-1]. 6 total.
- S_4: $\frac{\pi}{2}$ and $-\frac{\pi}{2}$ rotations around an axis followed by reflection in the plane of the axis. [1,0,0], [0,1,0] or [0,0,1]. 6 total.

Rotations are defined to be clockwise so minus rotations are counter clockwise. These symmetries are the elements of the group T_d. All elements can be represented by a unitary matrix working on basis vectors. To illustrate we will use the basis vectors x,y and z. Here we will present two examples: S_4 rotation around [1,0,0] and C_2 rotation around [1,0,0]:

$$S_4 = \begin{pmatrix} -1 & 0 & 0 \\ 0 & 0 & 1 \\ 0 & -1 & 0 \end{pmatrix} \quad \text{and} \quad C_2 = \begin{pmatrix} 1 & 0 & 0 \\ 0 & -1 & 0 \\ 0 & 0 & -1 \end{pmatrix}. \tag{A.1}$$

For a given set of symmetry operations A one can construct a set of matrices $D(A)$ that represents the operation, for a given basis, called an representation. The dimension of the representation is defined as the dimension of the matrices it contains. However the representations are not unique, because a shift of basis done by a singularity

transformation on the matrices will still be a representation of the same group. If a matrix $D(A)^i$ in a given representation can be transformed into block diagonal form by a similarity transformation its called reducible. If none of these blocks can be reduced further they are called irreducible. If any given similarity transformation would transform all the elements of a representation into the same block form, then the representation is reducible. Consider as a example two representations denoted by $D(A)$ consisting of 2 matrix elements of dimension 3:

$$D(A) = \left[\left(D(A)^1_{3\times3}\right), \left(D(A)^2_{3\times3}\right)\right] => S^{-1}D(A)S = B(A) = \left[\begin{pmatrix} B(A)^1_{2\times2} & \\ & B(A)^1_{1\times1} \end{pmatrix}, \begin{pmatrix} B(A)^2_{2\times2} & \\ & B(A)^2_{1\times1} \end{pmatrix}\right] \tag{A.2}$$

This reducible representation can be split into two irreducible representations (IRR) of dimensions 1 and 2. The matrices of a given IRR are not unique, but the traces of the contained matrices are, since a similarity transformation conserves the trace. The trace will be called the character χ of the representation.

The class is defined as a subgroup of elements in an IRR which are conjugate to each other, which means its elements must obey:

$$A = BCB^{-1} \tag{A.3}$$

Where A,B and C are elements of the same class. From this it is clearly seen that all elements in a class must have the same character, as B can be represented as a unitary matrix which conserves trace.

One of the central equations of group theory it what is known as Van Vleck's "Wonderfull orthogonality theorem" for IRR [10]:

$$\sum_A D^i_{\mu\nu}(A)D^j_{\mu'\nu'}(A^{-1}) = \frac{h}{l_j}\delta_{i,j}\delta_{\mu,\mu'}\delta_{\nu,\nu'} \tag{A.4}$$

Here the index i and j runs over different IRR's and l_j is the dimension of matrices in IRR j. h is the total number of elements in the group. Taking the trace of this, we obtain:

$$\sum_{A,\mu,\mu'} D^i_{\mu\mu}(A)D^j_{\mu'\mu'}(A^{-1}) = \sum_A \chi(A)^i\chi(A^{-1})^j = \frac{h}{l_j}\delta_{i,j}\sum_{mu,\mu'}\delta_{\mu,\mu'}\delta_{\mu,\mu'} = \delta_{i,j}h \tag{A.5}$$

Now since characters are the same for each class, we will now change summation so we sum over classes instead of elements. We also use $A^{-1} = A^*$.

$$\sum_k N_k\chi(k)^i\left[\chi(k)^j\right]^* = \delta_{i,j}h \tag{A.6}$$

Where k runs over the different classes of the IRR and N_k is the number of elements in each class. We will not proof it here, but this equation can be viewed as the dot product between two orthogonal basis vectors of length k. If there were one more IRR then k, we would have $k+1$ orthogonal vectors of k length which is not possible. If the length of k is less then the number of IRR, the vectors would not span the space, which is the same as saying that the set of IRR does not span the reducible representations. So the number of classes k must equal the number of IRR.

Rotations of the same angle around the same base consist of one class and reflections of the same base consist of another class. We therefore see that the point group T_d contains 24 elements divided into the 5 listed classes. There are therefore five IRR of the group T_d, which can be found by use of the orthogonality of classes:

$$\sum_i \chi(c)^i\left[\chi(k)^j\right]^* = \delta_{c,k}\frac{h}{N_k} \quad \text{and} \quad \sum_k \chi(k)^i\left[\chi(k)^j\right]^* N_k = \delta_{i,j}h \tag{A.7}$$

We will here list the IRR in a table, with their character corresponding to a given class, shown in what is known as Koster notation:

	E	$3C_2$	$6S_4$	6σ	$8C_3$
Γ1	1	1	1	1	1
Γ2	1	1	-1	-1	1
Γ3	2	2	0	0	-1
Γ4	3	-1	-1	1	0
Γ5	3	-1	1	-1	0

These IRR are the minimal basis that obeys all the symmetry operations. Since E is the identity operations it must consist of unit matrices. The trace of E is therefore equal to the dimension of the IRR.

The last thing we will talk about is basis vectors for the representations. Each IRR has a set of basis vectors of the same dimension as the IRR, which is the minimal group that generates the IRR from the symmetry elements. Suppose we have a group of symmetry operators A:

$$A\left|f^n,i\right\rangle = \sum_j D^n(A)_{ij}\left|f^n,j\right\rangle \tag{A.8}$$

where $|f^n,i\rangle$ is the i basis vector of the IRR denoted by n. Basis vectors belonging to different representations or different basis vectors of the same IRR are orthogonal. This can be shown using eqn.A.4. This means we can generate representations for symmetries using basis functions. We multiply the above equation with a different basis vector to get.

$$\left\langle f^m,a\right|A\left|f^n,i\right\rangle = \sum_j D(A)_{ij}\left\langle f^m,a|f^n,j\right\rangle = D(A)_{ia}\delta_{m,n} \tag{A.9}$$

This set of basis vectors is not a unique choice, but it will generate a unique representations of the group. The basis vectors are defined to be generators of the IRR. But if we choose a arbitrary non-basis vector sec we would generate a reducible representation. This representation could then be transformed to a IRR by a singularity transformation, which would change the arbitrary vectors into linear combinations of the basis vectors.

By using symmetry arguments we can deduce much about the wave functions of a given hamiltonian even before solving it. Since H must be invariant under any transformation that leaves the crystal invariant it must follow that:

$$H = A^{-1}HA \Rightarrow AH\left|\Psi_n\right\rangle = AE_n\left|\Psi_n\right\rangle \Rightarrow H\left|A\Psi_n\right\rangle = E_n\left|A\Psi_n\right\rangle \tag{A.10}$$

This shows that both $|\Psi_n\rangle$ and $|A\Psi_n\rangle$ are eigenvectors of H. So if we know one eigenfunction for a given energy, we can by using the symmetries construct additional eigenfunctions with the same energy. Consider now that we obtained a set of n degenerate eigenfunctions $|\psi,i\rangle$ with this method. Any linear combination of these functions would then be a eigenstate of the Hamiltonian, therefore we can write:

$$A\left|\psi^n,i\right\rangle = \sum_{j=1..n} D^n(A)_{ij}\left|\psi^n,j\right\rangle \tag{A.11}$$

Which is still an eigenstate of the Hamiltonian, but these states are also a generator for an IRR of the same dimension as the degeneracy. So for every degeneracy there must be a IRR of corresponding dimensions and the eigenvectors ψ must be basis vectors of the IRR. This important result lets us identify the degeneracies of the states using only symmetry. We can also conclude that any eigenvector for the hamiltonian can be reduced to linear combinations of basis vectors for the IRR.

B Tightbinding model

An easy way to visualize the different effects of the topological insulator is to use a tight-binding model [7]. The basis of tightbinding models is to substitute k_i with functions periodic with the lattice constant and only consider nearest neighbor interactions. We will use the usual substitution:

$$k_i = \frac{1}{a}\sin(k_i a) \quad \text{and} \quad k_i^2 = \frac{4}{a^2}\sin^2\left(\frac{k_i a}{2}\right) = \frac{2}{a^2}\left(2 - cos(k_i a)\right) \tag{B.1}$$

Its easy to verify that when k_i is close to zero we return to our old model. Now using these substitutions on the BHZ model and setting $C = 0$ we obtain:

$$H_{BHZ} = \left[-2\bar{D}(2-\cos(ak_x)-\cos(ak_y))\right]\sigma_0 + \left[M - 2\bar{B}(2-\cos(ak_x)-\cos(ak_y))\right]\sigma_z + \bar{A}\sin(k_x a) + \bar{A}\sin(k_y)\sigma_y \tag{B.2}$$

Here the bar indicates that the term is expressed in length scale of the lattice constant. We now shift basis and choose to express this in terms of creation and annihilation operators:

$$\Psi = \begin{pmatrix} a_{k_x,k_y} \\ b_{k_x,k_y} \end{pmatrix} \quad \text{and} \quad \Psi^* = \begin{pmatrix} a^\dagger_{k_x,k_y} \\ b^\dagger_{k_x,k_y} \end{pmatrix} \tag{B.3}$$

We will now adopt the of boundary conditions of a cylinder, which is periodic in x, so k_x is still a good quantum number, and with a open interface at both ends of the y axis. We must fourier transform our Hamiltonian back into real space along the y direction since k_z is not a good quantum number. The fourier transforms are:

$$c_j = \sum_k c_k e^{-ikaj} \rightarrow \frac{i}{2}(c_{j+1} - c_{j-1}) = \sum_k c_k \sin(ka) e^{-ikaj} \tag{B.4}$$

Now doing the fourier transformation on the BHZ model we obtain:

$$\langle \Psi^* | \, H \, | \Psi \rangle = \sum_j \left[H_{j,j} + H_{j+1,j} + H_{j,j+1} \right] \tag{B.5}$$

$$H_{j,j} = \left[-2\bar{D}(2 - \cos(ak_x)) \right] \sigma_0 + \left[M - 2\bar{B}(2 - \cos(ak_x)) \right] \sigma_z + \bar{A} \sin(k_x) \tag{B.6}$$

$$H_{j+1,j} = \bar{D}\sigma_0 + \bar{B}\sigma_z - i\frac{\bar{A}}{2}, \quad H_{j,j+1} = H^*_{j+1,j} \tag{B.7}$$

and any perturbation is transformed the same way. We can now use this model plot the BHZ model at different regimes. We use our parameters from our envelope function calculations over the HgTe quantum well.

References

[1] M. König et al., Science 318, 766 (2007).

[2] C. J.Wu, B.A. Bernevig, and S. C. Zhang, Phys. Rev. Lett. 96, 106401 (2006).

[3] M. G. Burt, J. Phys.: Condens. Matter 4, 6651 (1992)

[4] B. A. Foreman, Phys. Rev. B 56, R12 748(1997)

[5] Chaoxing Liu et Al, Phys. Rev. Lett, 100, 236601 (2008)

[6] A. Zakharova and S. T. Yen, K. A. Chao, Phys. Rev B 66, 085312 (2002)

[7] S. Shen, Topological Insulators. Berlin. Springer (2012)

[8] B. A. Bernevig and T. L. Hughes, Topological Insulators and Topological Superconductors. Princeton. Princeton University Press (2013)

[9] P. Y. Yu and M. Cardona, Fundamentals of Semiconductors. 3rd ed. Berlin. Springer (2005)

[10] M. S. Dresselhaus, Applications of Group Theory to the Physics of Solids. (2002)

[11] C. Galeriu $k \cdot p$ Theory of Semiconductor Nanostructures. Dissertation. Worchester Polytechnic Institute (2005)

[12] E. Halvorsen and Y. Galperin, K.A Chao, Phys. Rev. B 61, 16746 (2000)

[13] E. G. Novik et Al, Phys. Rev. B 72, 035321 (2005)

[14] D. Y. K. Ko and J. C. Inkson, Phys. Rev. B 38, 9946 (1988)

[15] M. Wada et Al. Phys. Rev. B 83, 121310 (2011)

[16] B. Chen, M. Lazzouni and L. R. Ram Mohan, Phys. Rev. B 45, 1205 (1992)

[17] A. T. Meney and Besire Gonul, Phys. Rev. B 50, 10894 (1994)

[18] T. B. Bahder, Phys. Rev. B 41, 11994 (1990)

[19] L. Du et al, arXiv:1306.1925v1 (2013)

[20] R. Winkler, Spin Orbit Coupling Effects in Two Dimensional Electron Hole Systems. Berlin. Springer (2003)

[21] A. V. Rodina et al, Phys. Rev. B 65, 125302 (2002)

[22] K. Suzuki, Y. Harada and K. Muraki, Phys. Rev. B, 87235311 (2013)